Development/Plasticity/Repair

AAV Vector Mediated Delivery of NG2 Function Neutralizing Antibody and Neurotrophin NT-3 Improves Synaptic Transmission, Locomotion, and Urinary Tract Function after Spinal Cord Contusion Injury in Adult Rats

Hayk A. Petrosyan,[1,2] Valentina Alessi,[1,2] Kristin Lasek,[1,2] Sricharan Gumudavelli,[2] Robert Muffaletto,[2] Li Liang,[1] William F. Collins III,[2] Joel Levine,[2] and Victor L. Arvanian[1,2]

[1]Northport Veterans Affairs Medical Center, Northport, New York 11768 and [2]Department of Neurobiology and Behavior, Stony Brook University, Stony Brook, New York 11794

NG2 is a structurally unique transmembrane chondroitin sulfate proteoglycan (CSPG). Its role in damaged spinal cord is dual. NG2 is considered one of key inhibitory factors restricting axonal growth following spinal injury. Additionally, we have recently detected its novel function as a blocker of axonal conduction. Some studies, however, indicate the importance of NG2 presence in the formation of synaptic contacts. We hypothesized that the optimal treatment would be neutralization of inhibitory functions of NG2 without its physical removal. Acute intraspinal injections of anti-NG2 monoclonal antibodies reportedly prevented an acute block of axonal conduction by exogenous NG2. For prolonged delivery of NG2 function neutralizing antibody, we have developed a novel gene therapy: adeno-associated vector (AAV) construct expressing recombinant single-chain variable fragment anti-NG2 antibody (AAV-NG2Ab). We examined effects of AAV-NG2Ab alone or in combination with neurotrophin NT-3 in adult female rats with thoracic T10 contusion injuries. A battery of behavioral tests was used to evaluate locomotor function. *In vivo* single-cell electrophysiology was used to evaluate synaptic transmission. Lower urinary tract function was assessed during the survival period using metabolic chambers. Terminal cystometry, with acquisition of external urethral sphincter activity and bladder pressure, was used to evaluate bladder function. Both the AAV-NG2Ab and AAV-NG2Ab combined with AAV-NT3 treatment groups demonstrated significant improvements in transmission, locomotion, and bladder function compared with the control (AAV-GFP) group. These functional improvements associated with improved remyelination and plasticity of 5-HT fibers. The best results were observed in the group that received combinational AAV-NG2Ab+AAV-NT3 treatment.

Key words: **Bladder Function; Locomotion; NG2; Proteoglycan; SCI; Transmission**

Significance Statement

We recently demonstrated beneficial, but transient, effects of neutralization of the NG2 proteoglycan using monoclonal antibodies delivered intrathecally via osmotic mini-pumps after spinal cord injury. Currently, we have developed a novel gene therapy tool for prolonged and clinically relevant delivery of a recombinant single-chain variable fragment anti-NG2 antibody: AAV-rh10 serotype expressing scFv-NG2 (AAV-NG2Ab). Here, we examined effects of AAV-NG2Ab combined with transgene delivery of Neurotrophin-3 (AAV-NT3) in adult rats with thoracic contusion injuries. The AAV-NG2Ab and AAV-NG2Ab+AAV-NT3 treatment groups demonstrated significant improvements of locomotor function and lower urinary tract function. Beneficial effects of this novel gene therapy on locomotion and bladder function associated with improved transmission to motoneurons and plasticity of axons in damaged spinal cord.

Received June 28, 2022; revised Jan. 6, 2023; accepted Jan. 10, 2023.

Author contributions: H.A.P., V.A., W.F.C., J.L., and V.L.A. designed research; H.A.P., V.A., K.L., S.G., R.M., L.L., W.F.C., J.L., and V.L.A. performed research; H.A.P., V.A., K.L., S.G., L.L., W.F.C., J.L., and V.L.A. analyzed data; H.A.P. and V.L.A. wrote the first draft of the paper; H.A.P., V.A., W.F.C., J.L., and V.L.A. edited the paper; J.L. contributed unpublished reagents/analytic tools; V.L.A. wrote the paper.

This work was supported by the Merit Review Funding from the Department of Veterans Affairs, Department of Defense, New York State SCIRB, and Craig H. Nielsen Foundation.

The authors declare no competing financial interests.

Correspondence should be addressed to Victor L. Arvanian at victor.arvanian@gmail.com.

https://doi.org/10.1523/JNEUROSCI.1276-22.2023

Introduction

Intracellular recordings from motoneurons and axons revealed injury-specific impairments of axonal conduction and reorganization of synaptic circuits after spinal cord injury (SCI) in rats (Arvanian et al., 2009; Hunanyan et al., 2013). Strengthening transmission/function at surviving connections is therefore a feasible approach to facilitate recovery after incomplete SCI. Abnormal accumulation of chondroitin sulfate proteoglycans

(CSPGs) (Snow et al., 1990) and insufficient neurotrophin support (Mendell et al., 2001; Schnell et al., 1994) are among the major reported obstacles known to restrict better recovery after SCI. CSPG molecules consist of a core proteins and side glycosaminoglycan (GAG) chains (Margolis and Margolis, 1993). Intraspinal injections of Chondroitinase-ABC (ChABC), an enzyme digesting the sugar chains of CSPGs (Yamagata et al., 1968), induced limited recovery of transmission in damaged spinal cord and transient improvements of motor function (Hunanyan et al., 2010). ChABC combined with neurotrophin NT-3 (Hunanyan et al., 2012; García-Alías et al., 2011) or prolonged administration of ChABC (Bartus et al., 2014) induced better recovery. A potential disadvantage of the use of ChABC is that it is not specific (i.e., it degrades all CSPGs by removing chondroitin sulfate GAG side chains) (Moon et al., 2001). CSPGs, however, are essential components of the extracellular matrix and are involved in many CNS functions, including modulation of axonal growth and synapse formation (Dityatev et al., 2010; Kwok et al., 2012). Therefore, targeting a single CSPG family member has been proposed to be more beneficial than degrading all CSPGs (Zhou et al., 2001; Brakebusch et al., 2002; Bartus et al., 2014).

Among the CSPGs elevated in the vicinity of the glial scar, neuro-glial-2 (NG2) has been implicated as a major obstacle to axonal regeneration (Levine, 1994; Jones et al., 2002). NG2 is a structurally unique transmembrane proteoglycan with a core protein of ~300 kDa and at least one side GAG chain (Nishiyama et al., 1991; Stallcup, 2002). The extracellular part of the core protein has three distinct domains that interact with a large number of proteins, which gives NG2 distinct functional modules.

We recently discovered new inhibitory function of NG2, i.e., blocking axonal conduction: exogenous NG2 induced acute block of axonal conduction, but other CSPGs tested did not (Hunanyan et al., 2010). Consistent with these effects of NG2 on axonal conduction, we and others found that NG2-positive processes contact nodes of Ranvier within the nodal gap, at the location of nodal Na-channels (Petrosyan et al., 2013) which are known to be directly involved in propagation of action potentials (APs) along spinal axons (Wang et al., 1997; Black et al., 2006).

We have recently examined the physiological effects of a monoclonal NG2-antibody-69 (NG2-Ab) known to bind to the N-terminal domain three of the NG2 core protein proteoglycan and prevent its inhibitory effects on axonal growth (Ughrin et al., 2003). We have demonstrated that NG2-Ab did not induce any changes in physiological properties of axons or neurons when injected intraspinally into naive animals. NG2-Ab did, however, prevent the conduction block induced by acute intraspinal injections of NG2 (Petrosyan et al., 2013). Intrathecal infusion of NG2-Ab, via osmotic mini-pump for 2 weeks, improved locomotor function following lateral hemi-section SCI. The effect of infused NG2-Ab on Basso-Beattie-Bresnahan (BBB) locomotor score, however, was limited and the improvements seen during the first 3 weeks were not sustained beyond 1 week following the conclusion of antibody infusion (Petrosyan et al., 2013). In the current study, we sought to examine a prolonged and clinically relevant method of NG2 neutralization. We investigated the use of adeno-associated virus (AAV) vector mediated delivery of a recombinant single-chain variable fragment (scFv) of the anti-NG2 antibody (AAV-NG2Ab). We assessed transduction efficiencies of AAV-NG2Ab in a mid-thoracic contusion SCI model of adult rats. We have examined effects of AAV-NG2Ab alone or in combination with AAV-NT3 on synaptic transmission, locomotor function, anatomic plasticity, and bladder function following SCI.

Some of these findings have been presented in abstract form (Arvanian et al., 2016).

Materials and Methods

Design of experiments

All experiments were conducted on adult, female, Sprague Dawley rats (~210-250 g) and performed in compliance with Institutional Animal Care and Use Committee policies at Stony Brook University and the Northport VA Medical Center. Animals were pretrained for behavioral tests and randomly divided into experimental groups to evaluate effects of treatments on transmission, motor, and bladder function. Randomly chosen animals from each group were used in experiments involving immunohistochemistry and electron microscopy to evaluate effects of treatment on anatomic changes. Animals in the sham group received sham laminectomy and intraspinal injections of AAV-GFP but no injury. Control SCI groups received T10 contusion injury and intraspinal injections of AAV-GFP (AAV-GFP). AAV-NG2Ab only group received the same T10 contusion injury and intraspinal injections of AAV-NG2Ab (described below) immediately following injury. The combination group (AAV-NG2AB+AAV-NT3) received the same T10 SCI and intraspinal injections of both AAV-NG2Ab and AAV-NT3 together immediately following injury. Since we previously found that the AAV-NT3 treatment group did not show significant improvements in locomotor function (Petrosyan et al., 2015); an AAV-NT3 alone group was not used in this set of experiments. Since we have also previously demonstrated that SCI and no treatment and SCI injected with AAV-GFP show no difference in locomotor performance (Petrosyan et al., 2015), here we have used the AAV-GFP group only as control for SCI. After SCI and AAV administration, animals were evaluated for locomotor recovery and bladder function for 9 weeks after which terminal electrophysiology, anatomic tracing, immunochemistry, or electron microscopy experiments were performed. Behavioral testing protocols were performed weekly. After completion of behavioral testing, each group (20-24 rats/group; 12-14 rats per group for motor/withdrawal tests and 8 rats per group for evaluation of bladder function) was divided into three subgroups. All selections were made randomly. One group was used for terminal electrophysiology to examine transmission, a second group for electrophysiology to examine cystometry/bladder function, and a third group for injection with anatomic tracers with termination 2 weeks later. After completion of electrophysiological and tracing experiments, rats were intracardially perfused and spinal cords prepared for evaluation of injury extent, confirmation of treatment delivery, immunochemistry, and confocal and electron microscopy. Experimenters were blind with regard to AAV-based treatment received throughout all phases of the experiment. Consistency of the injury was examined in all rats by evaluating their locomotor performance in Open Field (BBB score) (Basso et al., 1996) 2 d after operation. Animals that showed very mild or very severe impairment of hindlimb function compared with others were excluded and new animals were added instead (usually ~5% of animals).

Spinal cord injuries and treatment delivery

Animals were deeply anesthetized in induction chambers with 3% isoflurane in 100% O_2, and then transferred to a face mask delivering 1.5% isoflurane in 100% O_2 to maintain an anesthetic state during surgeries. Rats received subcutaneous injections of buprenorphine (0.01 mg/kg) to control postsurgical pain. Injuries were performed at the T10 spinal level using an IH-0400 impactor device (Precision System and Instrumentation). After performing dorsal laminectomy to expose the T10 spinal cord, vertebral bodies rostral and caudal to the opening were fixed to stabilize the spinal cord. The impactor probe (2.5 mm diameter) was positioned 1 mm above the dorsal surface of spinal cord, in the center of the opening, and 150Kdyn force was delivered (as in Petrosyan et al., 2014). Immediately after the injury and visual inspections of injury epicenter, animals received

intraspinal injections of vectors expressing either GFP as a control or NG2Ab and neurotrophin NT3 administered alone or together. Intraspinal injections were performed as previously described by Petrosyan et al. (2014). Briefly, two intraspinal injections (1 µl each) were made into spinal cord on the midline, 1.5 mm rostral and caudal from injury epicenter, at 1 mm depth. Our recent experiments demonstrated strong transduction of both neurons and glial cells in the contused spinal cord following similar injections of AAV-GFP (Petrosyan et al., 2014). Following the injury and AAV injections, muscles were sutured and skin was closed with surgical clips followed by subcutaneous injections of antibiotic (Baytril 5 mg/kg) and 5 ml of sterile lactated Ringer's solution. Animals received injections of carprofen (5 mg/kg) and lactated Ringer's for 3 d after surgery and then as needed.

AAV vectors and NG2 antibody production

We have recently constructed an scFv from anti-NG2 monoclonal antibody 69 (Ughrin et al., 2003). Antibody 69, an IgG2a, is directed against the C-terminal Domain 1 of the NG2 core protein and recognizes the shed extracellular domain of the NG2 core protein. The antibody neutralizes the growth-inhibitory activity of NG2 in *in vitro* neurite outgrowth assays (Ughrin et al., 2003). Total RNA from monoclonal 69 hybridoma cells was isolated by TRIZOL RNA extraction (Invitrogen) and treated with RNase-free DNase (TURBO DNA-free; Ambion) following the protocols of the manufacturers. RNA concentrations were measured using a NanoDrop 1000 spectrophotometer, and 250-300 ng of total RNA was used for reverse transcription with Superscript II Reverse Transcriptase (Invitrogen) via the protocol of the manufacturer. Heavy and light chain variable regions were amplified using Ig-primer sets (Novagen) and cloned into Perfectly Blunt cloning vectors (Novagen). The resulting vectors were transformed into Bluescript II KS phagemid vectors (Stratagene) and positive clones selected by blue/white screening. Positive clones were identified by DNA sequencing and an artificial gene constructed (Integrated DAN Technologies). The gene contained a 5′ heavy chain leader, cloned Vh, a linker region (GGGS), cloned Vl, and a 6-His tag. The artificial gene was inserted in AAA rh.10 (AAVrh10.CB7.CI.69Svig.WPRE.rBG, Penn Vector Core, University of Pennsylvania; 4.23×10^{12} GC/ml dosage) . Expression of the anti-NG2 svFc was confirmed by infection of HEK 293T cells and Western blots of media and cell lysates with anti-6His antibodies (NeuroMab). Other AAV serotype rh.10 vectors used in this study were: encoding the GFP gene (AAVrh10.CMV.PI.eGFP.WPRE.bGH; 3.99×10^{12} GC/ml dosage) and NT-3 gene coexpressing GFP gene (AAVrh10.CMV.bGHint.NT3.IRES.EGFP.WPRE.bGH; 4.6×10^{12} GC/ml dosage). Production, packaging, and purification of all these viral vectors were performed by Penn Vector Core at the University of Pennsylvania.

Behavioral assessment

Before injuries, all animals were handled and acclimatized for all behavioral tests and pre-injury scores were taken.

Open field BBB score. Open field BBB scoring was used to assess locomotor function. Joint movements, weight support, paw placement, and coordination were evaluated according to the 21-point BBB locomotion scale by two observers as previously described (Basso et al., 1996).

Irregular grid. Animals were evaluated as they crossed a 1-m-long horizontal ladder (bars placed randomly ~1-4 cm apart) elevated from the ground. The middle part of the ladder (~60 cm) was used for scoring. The number of foot slips from three trials was counted and normalized by the total number of steps for each animal as previously described (Arvanian et al., 2009; Petrosyan et al., 2015).

Narrowing Beam. Progressively Narrowing Beam with a length of 1.5 m was used to evaluate the locomotor function as previously described (Petrosyan et al., 2015). Briefly, the entire length of the beam is divided into 30 numbered equal units with 50 mm width at the beginning and 10 mm at the termination. The unit at which the first slip of hindlimbs was made was recorded for each rat and normalized for three runs.

Catwalk gait analysis. Gait print parameters were assessed using CatWalk system (Noldus Information Technology). Animals crossed a glass runway where their footprints were captured by a high-speed camcorder. For each rat, data from three complete runs were collected and analyzed using CatWalk XT software (Hamers et al., 2001; Petrosyan et al., 2013). Coordination and other gait parameters, such as Base of Support and Stride Length, were analyzed and compared between experimental groups as previously described (Petrosyan et al., 2013).

Withdrawal reflexes. The thermal nociceptive threshold for both hind paws was evaluated by performing a standardized plantar heater test (Hargreaves et al., 1988) using a commercially available apparatus (Hot/Cold Plate, Bioseb). Rats were placed in a Plexiglas box (17 × 23 cm) and allowed to adjust. After animal calms, an infrared source producing a calibrated heating beam (diameter 1 mm) was placed under the hind paw and triggered together with a timer. There was a minimum 30 s interval between trials. In addition, von Frey hairs (EB Instruments) with target force ranging from 0.008 to 300 g was used. Rats were placed in a Plexiglas box with a fine grid bottom and allowed to adjust. The monofilament was pressed against the plantar surface of the foot at a 90° angle until it bows, and held in place for 1-2 s. This was repeated up to 3 times in the same location. The test was performed by using increasing filament calibers until the first withdrawal reflex was noted. Details were described by Schnell et al. (2011).

Bladder function evaluation

Lower urinary tract function was assessed during the survival period using metabolic chambers to collect and quantify overnight urine production, and then after 6 weeks, during terminal cystometry recordings with simultaneous acquisition of external urethral sphincter (EUS) activity and bladder pressure. Analysis included bladder pressure threshold and peak bladder pressure during contractions, intermicturition interval, void volume, residual volume, duration of EUS bursting, and amplitude and duration of EUS activity.

Metabolic chambers. Micturition patterns were measured weekly using UroVoid system for noninvasive measurements of bladder function in conscious rats (Med Associates). Animals were placed into metabolic chambers, designed to separate feces from urine, for a period of 15 h overnight with a libitum access to food and water, and urine was collected into glass flasks placed on analytical balances for accurate void mass quantification. The balances were connected to a computer where data were measured and stored using UroVoid system (Med Associates). Offline analysis was performed using Igor Pro 6.34A, UOMA 3.0.2 software and included calculation of the number of voids, mean time between voids (intercontraction interval), mean volume per void, and total urine output during the dark cycle. Micturition pattern data were collected from each rat weekly beginning from week 2 after injury and continuing until the final cystometry experiments.

Cystometry. Cystometry procedures were described previously in (D'Amico et al., 2011; D'Amico and Collins, 2012). Briefly, animals were anesthetized with urethane (1.2 g/kg, IP and then supplemented if needed), and a heating pad was used to maintain animal body temperature at 37°C throughout surgery. Heart rate was monitored continuously. Following an incision in the neck, a cannula was inserted into either the left or right internal jugular vein for fluid administration and a trachea tube was inserted to facilitate respiration. Following a midline incision made into the lower abdomen, the pubic symphysis was removed to expose the underlying EUS muscle. A midline abdominal incision through skin and musculature was performed to expose the bladder. A pursestring suture (4–0 Ethilon) was placed into the urothelium of the bladder dome. PE-90 tubing (for which the tip was previously heated to shape a collar ~2 mm from the end) was then inserted through the bladder dome within the suture limits and secured. This tubing was then attached to an infusion pump and pressure transducer. Insertion of a flared ended tube into the bladder dome was performed and then connected to a pressure transducer to measure intravesical pressure (BP) and to a syringe pump for room temperature 0.9% saline infusion (up to 21 ml/h). Data were analyzed offline using the IGOR pro/NIDAQmx Tools (WaveMetrics). At the conclusion of the experiment, an overdose of urethane was administered intravenously to euthanize animals.

Electrophysiological evaluation of transmission

Animals dedicated for electrophysiological evaluation of synaptic transmission or axonal excitability were deeply anesthetized using a ketamine/xylazine mixture for terminal experiments. Intracellular and intra-axonal recordings performed in this study are described in detail (Arvanian et al., 2009; Hunanyan et al., 2011; Petrosyan et al., 2013). Briefly, after initial induction using 3% isoflurane in 100% O_2 in an induction chamber, animals received intraperitoneal injections of a ketamine/xylazine (80 mg/kg/10 mg/kg) mixture for induction and were supplemented during experiment with 1/5 initial dose injected intramuscularly if needed. An automatically controlled heating pad was used to maintain animal body temperature at 36.7°C, and expired CO_2 and heart rate were continuously monitored during experiment. For placement of stimulation electrode, dorsal laminectomies were performed at T5-T7 spinal cord. Dorsal laminectomies at lumbar L1-L6 spinal levels were performed and clamped with custom-made metal bars to stabilize the cord for intracellular recordings (Petrosyan et al., 2013).

Intracellular recordings. Intracellular recordings (Axoprobe amplifier: Molecular Devices) were recorded from L5 spinal cord using sharp, glass microelectrodes (3 M K-acetate) with 50-70 MΩ resistance. Responses were evoked by electric stimulation of lateral white matter (LWM) tracts at T6 rostral as described previously (Arvanian et al., 2009; Hunanyan et al., 2012). Pulsemaster A300 with Isolator unit A360 (World Precision Instruments) was used for electrical stimulation, a tungsten stimulation electrode (FHC, resistance: 300 kΩ) was placed in T6 LWM to stimulate fibers located in ventrolateral funiculi. Using a micromanipulator, the electrode was positioned between the dorsal root entry zone and lateral edge at 25° angle and lowered to the depth of 1.7 mm as previously described (Arvanian et al., 2009; Hunanyan et al., 2011).

Intra-axonal recordings. Intra-axonal recordings (Axoprobe amplifier; Molecular Devices) were performed from lateral white-matter axons at L1 level using custom pulled glass microelectrodes (3 M K-acetate) with 25-50 MΩ resistance, as previously described (Hunanyan et al., 2011; Petrosyan et al., 2013). Active bridge circuit recording mode (Axoprobe amplifier; Molecular Devices) was used to allow simultaneous recording and current injection through the same electrode. Axons were identified by drop of membrane potential, no changes in amplitude of AP amplitude when the stimulus intensity was changed, and no underlying synaptic potential (Kocsis and Waxman, 1982). Axons with membrane potentials more negative than ~55 mV were used for analysis.

Extracellular recordings. Extracellular responses were recorded from right L5 ventral horn gray matter as described previously (Hunanyan et al., 2012; Petrosyan et al., 2015). Briefly, recordings were performed via tungsten electrode (resistance 300 kΩ; FHC) that was lowered to a depth of 1.3 mm and positioned at the dorsal root entry zone with an angle of 25° from vertical in the sagittal plane as described before (Arvanian et al., 2009). Extracellular responses were recorded in response to electric stimulation of LWM at T6 spinal level as described above. All signals were amplified, filtered, and recorded using Digidata 1550B digitizer (Molecular Devices) and analyzed offline using pCLAMP 10 software (Molecular Devices).

Biotin dextran amine (BDA) tracing

A subgroup of animals dedicated for axonal tracing experiments was anesthetized with isoflurane as described above. The scalp was shaved, and the area was treated with alcohol and betadine. Small holes were drilled in the skull over the sensorimotor cortex (SMC), and a Hamilton syringe clamped to micromanipulator was used to inject the anterograde tracer BDA (10,000, Invitrogen) into the SMC (2 mm posterior to bregma, 2 mm lateral to bregma at the 1.5 mm depth) as described previously (Fouad et al., 2001; Bareyre et al., 2004; García-Alías et al., 2011). After completing the injections, the skin was closed and analgesics and antibiotics were administered as described above. Two weeks after injections, rats were perfused, and spinal cords were prepared for evaluation. Cervical C1-C4 transverse sections were incubated in ABC elite reagent kit (Vector Laboratories) overnight at 4°C followed by incubation with TSA Fluorescein System (PerkinElmer) to visualize BDA filled axons. Total area of positive BDA fibers in gray matter was quantified using ImageJ software from images collected with a Zeiss Axioskop2 microscope with an AxioCam MRm camera (Carl Zeiss). The time frame of 2 weeks for tracer experiment was chosen for two reasons: (1) it usually took ~2 weeks per group to complete electrophysiological evaluation, which allowed us to draw parallels between electrophysiology and tracing experiments; and (2) a survival time of 2 weeks after BDA injections has been widely used in the literature (Fouad et al., 2001; Bareyre et al., 2004), including our own study (García-Alías et al., 2011), allowing us to compare results of the current study with literature data. C1-C4 areas were chosen for analyses based on previous results demonstrating that most innervation of cervical cord by collaterals of corticospinal tract fibers originating from hindlimb sensory motor cortex (2 weeks after BDA injections) has been observed at C2-C3 and neighboring cervical levels following thoracic SCI (Fouad et al., 2001).

Tissue processing

Immunohistochemistry and image analysis. At the end of experiments, animals were transcardially perfused with 400 ml of 4% PFA in 0.1 M PBS and spinal cords were removed for processing. After perfusions, spinal cords were postfixed overnight in 4% PFA followed by cryoprotection for a minimum of 48 h in a 30% sucrose solution. Spinal cord segments were sectioned on a cryostat (Microm HM550, Fisher Scientific) and collected serially onto Colorfrost Plus slides (Fisher Scientific) in five sets. Transverse sections were cut at 40 µm thickness and horizontal sections were cut at 20 μm thickness. One set of alternating serial sections was stained with Cresyl violet (Petrosyan et al., 2014) and used for injury reconstruction and to determine spinal cord segment levels.

Staining to visualize NG2-AB delivery. One set of alternating sections was used to evaluate and visualize NG2 antibody delivery. Immunofluorescence staining for 6-HIS (rabbit anti-6His, 1:100, Abcam) was used to visualize delivered antibody (NG2-Ab/6-His tag). In addition, sections were double-immunostained with NeuN, CC-1, and ED-1 to see transduction tropism of AAV vector. For double immunofluorescence staining, sections were incubated in primary antibodies mouse anti-NeuN (1:100, Millipore), mouse anti-CC-1 (1:100, Abcam), and mouse anti-CD68(ED-1) (1:200, Abcam) overnight at 4°C followed by three washes in 0.1 M PBS (3 × 10 min). For double immunostaining with NG2, mouse anti-6His (1:3, Neuromab) and rabbit anti-NG2 (1:500) primary antibodies were used. Sections were then incubated in appropriate secondary antibodies (goat anti-mouse AlexaFluor-488 and goat anti-rabbit AlexaFluor-594 [1:800]) for 2 h at room temperature. Slides were washed in PBS, rinsed briefly in DH_2O, and coverslipped with Fluoromount-G (Southern Biotechnology). Images were taken with Zeiss Axioskop 2 Plus fluorescence microscope and used for further image analysis.

Staining with CASPR and NG2 to locate NG2-positive processes within nodes of Ranvier. Double immunofluorescence staining for Caspr and NG2 was conducted on one set of alternating serial sections. Sections were blocked for 1 h in 6% normal goat serum in 0.1 M PBS with 0.3% Triton X-100, then incubated in primary antibodies (mouse anti-Caspr [1:1000, NeuroMab] and rabbit anti-NG2 [1:500]) followed by incubation in AlexaFluor (Invitrogen) goat anti-mouse 594 (1:800) and goat anti-rabbit 488 (1:800) secondary antibodies as described above. To quantify the number of nodes containing NG2-positive processes, four fixed areas from white matter (two bilateral areas rostral and two bilateral areas caudal to injury) were used for analysis.

Staining with myelin basic protein (MBP) to see effects of treatment on myelination. Immunofluorescence staining for MBP was performed on one set of sections to determine effects of treatment on myelination. Primary antibody used was chicken anti-MBP (1:100, Millipore) followed by incubation with secondary goat anti-chicken AlexaFluor-488 (1:800, procedures described above). To quantify the changes in myelination, we calculated and compared the thresholded pixel mean intensities of MBP signal in white matter (20 sections per animal, $n = 12$) using ImageJ software (as described by Tom et al., 2009; Petrosyan et al., 2013).

Staining with 5-HT to visualize 5-HT fibers. One set of sections was used for immunofluorescence staining for 5-HT-positive fibers. The primary antibody used was rabbit anti-5HT (1:1000, Immunostar), followed by incubation in secondary antibody goat anti-rabbit AlexaFluor-594 (1:400, procedures described above). To measure the effects of treatment on 5-HT-positive fibers, ImageJ software was used to calculate the total area of 5-HT-positive immunoreactivity in ventral horns of 20 sections per animal ($n = 12$) from L1-L5 spinal segments. Detailed description of 5-HT immunostaning in lumbar segments of SCI animals has been previously described (Tom et al., 2009; Hunanyan et al., 2013; Petrosyan et al., 2013).

Electron microscopy

Procedures for tissue processing and electron microscopy analysis were performed as described previously (Pearse et al., 2005; Hunanyan et al., 2011). Briefly, rats were perfused with 4% PFA/2.5% EM grade glutaraldehyde in 0.1 M PBS. Spinal cords were removed, postfixed overnight, and L1-L2 segment removed and sectioned on a Vibratome at a thickness of 50 μm. Samples used for transmission electron microscopy were processed using standard techniques. Briefly, samples were then placed in 2% osmium tetroxide in 0.1 M PBS, pH 7.4, dehydrated in a graded series of ethyl alcohol and embedded in Durcupan resin. Ultrathin sections of ~80 nm were cut with a Leica EM UC7 ultramicrotome and placed on formvar-coated slot copper grids. Sections were then counterstained with uranyl acetate and lead citrate and viewed with a FEI Tecnai12 BioTwinG2 electron microscope. Digital images were acquired with an AMT XR-60 CCD Digital Camera system. G-ratio calculations were performed as described previously (Arvanian et al., 2009). Analysis was performed on a total of 500-600 axon profiles randomly imaged from ventral and LWM of L1 spinal segment for each rat ($n = 4$ per group).

Statistical analysis

Statistical analysis was performed using SigmaPlot 11.0 software (Systat Software). A *t* test, one-way ANOVA, or one-way ANOVA on ranks followed by Tukey's multiple comparisons *post hoc* test was used to compare the groups. Data are presented as mean ± SE. $p < 0.05$ is considered statistically significant.

Results

Verification of treatment delivery

One goal of this study was to confirm transgene delivery of NG2 function neutralizing antibody to the injury penumbra, where the level of NG2 proteoglycan is elevated the most (Fidler et al., 1999; Jones et al., 2002; Andrews et al., 2012). The choice of AAV10 serotype for transgene delivery of NG2-Ab and NT-3 was based on our previous studies showing that the same AAV10 vector induced robust transduction of both neuronal and glial cells in identical models of chronically contused rats (Petrosyan et al., 2014). Compared with other AAV serotypes tested, AAV10 induced robust transduction of not only neurons, but macrophages/microglia, oligodendrocytes, and NG2-positive cells (most probably oligodendrocyte precursor cells [OPCs]). Spinal cord neurons transduced by AAV10 distant from the intraspinal injections site showed transduction of neurons as far as at T2 thoracic and L5 lumbar levels. One separate group of SCI animals that received AAV-NG2Ab+AAV-NT3 treatment was used to confirm treatment delivery and tissue transduction with AAV vectors ($n = 5$). Four weeks after injury and vector injection, animals were perfused and tissue was processed for immunohistochemistry and electron microscopy to evaluate transduction efficacy, area of transduction, and cellular tropism of viral vectors. Results revealed many transduced cells and processes immediately in the vicinity of injury as well as evidence of transduction in areas of the spinal cord more remote from the injection site.

In accordance with our previous results (Petrosyan et al., 2014), gene expression was concentrated to the injection site and declined with distance; however, there were detectable stable signals in distant parts of the cord. Figure 1*A*, *B* shows the overall pattern of gene expression for NT3 (Fig. 1*A*, green signal) and NG2-Ab (Fig. 1*B*, red signal) at the injury epicenter (T9-T11). Higher-magnification images of gray matter at the T9-T11 level demonstrate that many cells were transduced with the AAV vectors, either individually or together (Fig. 1*C–E*, thin arrows). Electron microscopy experiments performed on sections from T9-T11 spinal segments confirm expression of NG2-Ab in cells (Fig. 1*F*). Figure 1*G* shows axons with signal close to injury epicenter.

To determine the type of cells that expressed NG2Ab after AAV-mediated delivery, we conducted immunostaining for 6-His tag, which was incorporated into the scFv DNA. As shown in Figure 2, double immunostaining with anti-6-His (to detect AAV-mediated delivery of NG2Ab) and oligodendrocyte marker CC-1 (Fig. 2*A*), neuronal marker NeuN (Fig. 2*B*), or macrophage marker ED-1 (Fig. 2*C*), show different cell types expressing NG2-Ab after viral delivery into the injured spinal cord: that is, oligodendrocytes, including lateral and ventrolateral white matter close to contusion; neurons in gray matter caudal/rostral to injury; and importantly microglia/macrophages at the injury epicenter. Other double immunolabeling experiments revealed (1) many NG2-positive cells (most probably OPCs) and processes, and (2) AAV-mediated delivery of NG2-Ab (traced with 6-HIS) in close proximity to these NG2-positive cells and processes in the LWM close to the contusion level (Fig. 2*D*).

Treatment with AAV-NG2Ab and AAV-NT3 improved locomotor function

To assess the effects of treatments on locomotor function, animals were evaluated weekly with a set of behavioral tests, including BBB locomotor score (Fig. 3*A*), Narrowing Beam (Fig. 3*B*), and Irregular Ladder (Fig. 3*C*) challenging tests, as well as Catwalk automated gait analysis (Fig. 3*D–F*). During the first 2 weeks after injury, animals did not show stable hindlimb weight support; thus, Catwalk assessment was started 2 weeks after injury. All three groups showed similar deficits after injury during the first 2 weeks (Fig. 3), thus suggesting consistency of the injury severity among groups/animals.

CatWalk and BBB scoring

As shown in Figure 3, beginning from week 3, both AAV-NG2-Ab ($n = 12$) and AAV-NG2AB+AAV-NT3 treatment groups ($n = 12$) showed a significantly higher number of coordinated steps, as evidenced by a higher regularity index assessed by CatWalk, compared with the AAV-GFP group ($n = 12$; $p < 0.0$ 5). At week 3, all groups, however, demonstrated similar BBB scores, and improvements in these two treatment groups have been detected beginning from week 4 (Fig. 3). These results provide additional evidence demonstrating that more sensitive tests, such as Catwalk gait analysis, provide a more sensitive assessment of recovery of function that is not detectable by conventional tests, such as BBB (Koopmans et al., 2005). Other gait parameters assessed with CatWalk system, such as Base of Support of hind limbs and Stride Length of forelimbs, were also significantly better in AAV-NG2Ab and AAV-NG2AB+AAV-NT3 groups beginning from week 4 after treatment administration compared with AAV-GFP group ($n < 0.05$).

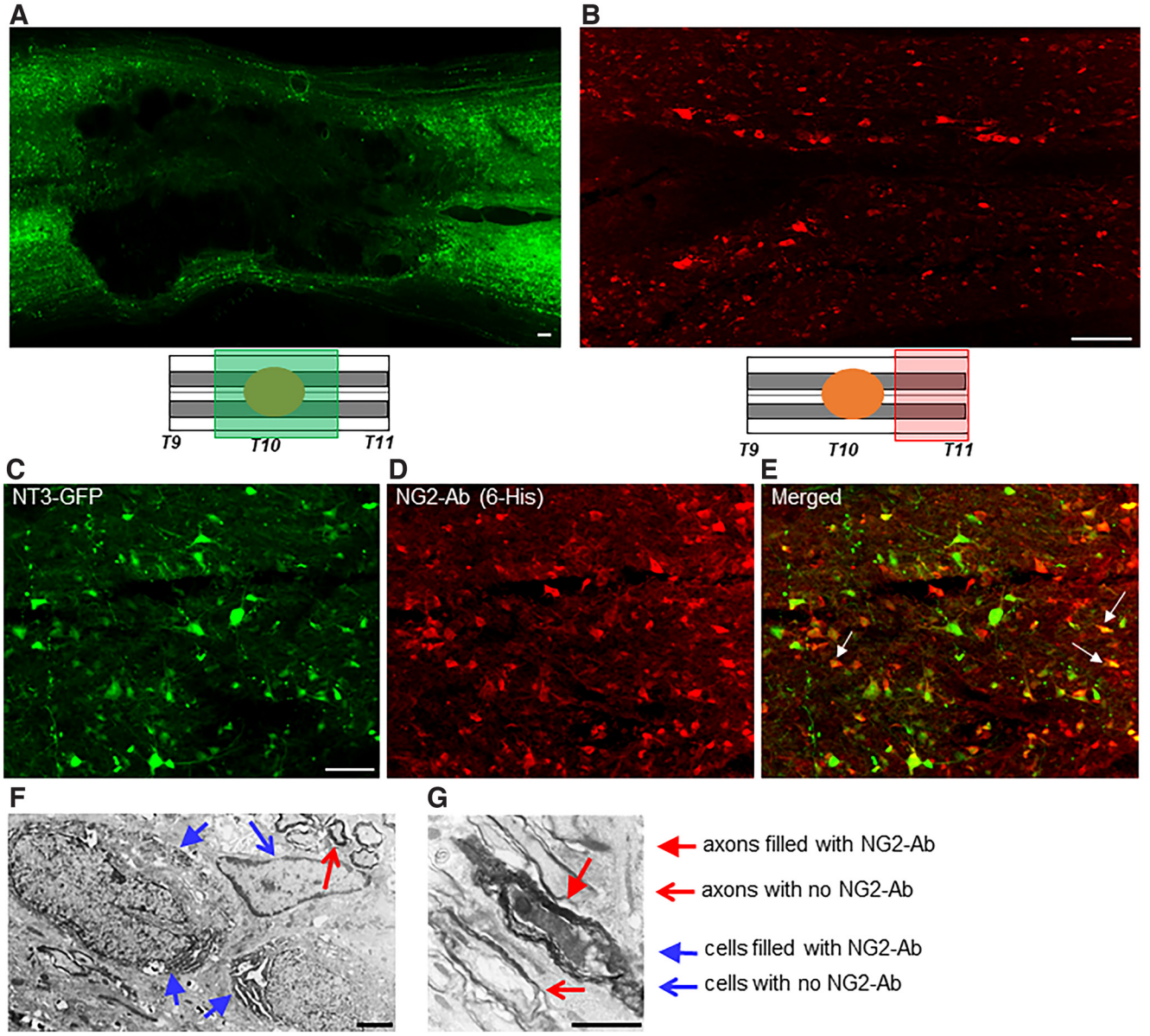

Figure 1. Robust transduction of spinal cord tissue following intraspinal injections of AAV-NT3 and AAV-NG2Ab. ***A***, ***B***, Horizontal sections of T9-T11 spinal segments. GFP signal was used to visualize AAV-mediated delivery of NT3 coexpressing GFP (***A***, green) and immunostaining with anti-6-His to detect 6-His-tagged NG2-Ab (***B***, red). Diagrams represent the area where high-power images were taken. ***C–E***, High-magnification images of the gray matter close to injury epicenter demonstrating GFP signal (***C***) and anti-6-His-stained sections (***D***) represent many transduced cells with NT3-GFP and NG2Ab. ***E***, Merged image represents colocalization of NT3 and NG2-Ab in many cells (arrows). ***F***, ***G***, Electron microscope images confirm expression of NG2-Ab in cells (***F***) and axons (***G***) in AAV-NG2Ab-injected rats. Arrowheads point to cells and fiber with no 6-His signal. Filled arrowheads point to cells and a fiber transduced with AAV-NG2Ab. Scale bars, 2 μm.

Narrowing Beam and Irregular Ladder tests

Beginning from weeks 4-5, rats from both AAV-NG2Ab and AAV-NG2Ab+AAVNT3 groups demonstrated significantly better performance in both Narrowing Beam (Fig. 3*B*; $p < 0.05$) and Irregular Ladder (Fig. 3*C*; $p < 0.05$) challenging tests, as demonstrated by longer distance passed in Narrowing Beam and fewer number of slips on Irregular Ladder, compared with the AAV-GFP group ($p < 0.05$).

Improved locomotor function sustained for the reminder of the testing period for both groups in all tests and was still significantly better compared with other groups at the conclusion of behavioral tests at week 9 (Fig. 3). Importantly, starting from week 5, rats from the combination treatment group, AAV-NG2AB+AAV-NT3, exhibited better performance in almost all tests, including BBB Score, Narrowing Beam, Irregular Ladder, Catwalk Regularity Index, Catwalk Base of Support and Catwalk Stride Length, compared with not only control AAV-GFP but also Group treated with AAV-NG2Ab only (Fig. 3; $^{**}p < 0.05$).

Withdrawal reflex was examined after completion of the motor tests at week 9 after injury to minimize interference with the motor tests. Withdrawal reflex, which was evaluated using both von Frey threshold filament strength (Fig. 3*G*) and Hargreaves withdrawal latency (Fig. 3*H*), was not significantly affected by these treatments. Data are presented as mean ± SE; $p = 0.9$ and 1.4, respectively.

Treatment with AAV-NG2Ab+AAV-NT3 improved bladder function

To assess bladder function, we used metabolic chambers weekly and assessed the micturition pattern overnight during the survival period, starting 2 weeks after injury. At the end of survival

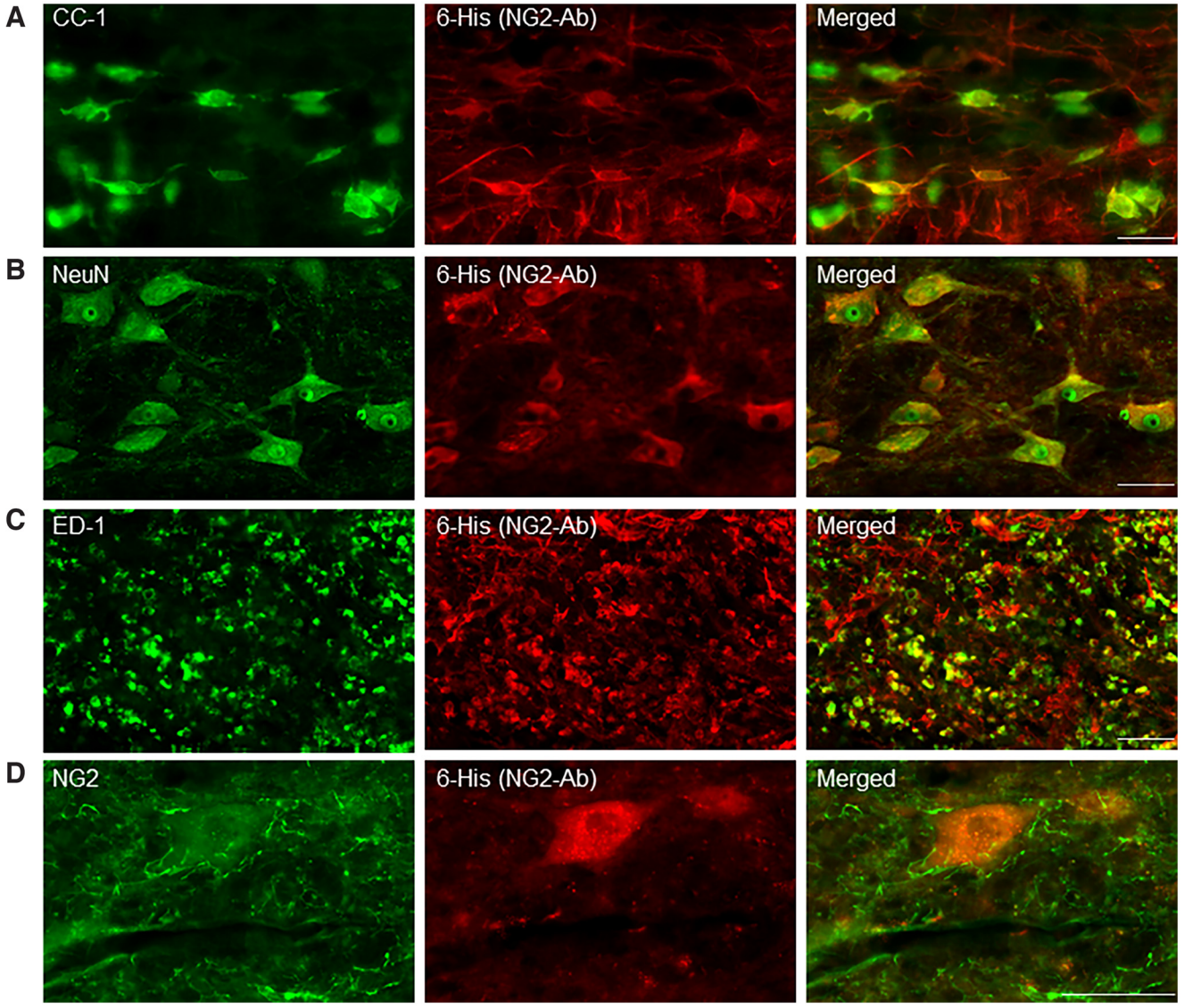

Figure 2. Transduction of different types of cells following intraspinal injections of AAV-NG2Ab in injured spinal cord. Images from T9-T11 horizontal sections of T10 contused spinal cord taken in the LWM caudal to injury at depth corresponding to VLF. Double immunostaining with anti-6-His (red, to detect AAV-mediated delivery of NG2Ab) and oligodendrocyte marker CC-1 (***A***), neuronal marker NeuN (***B***), and macrophage marker ED-1 (***C***). ***D***, Double immunostaining with NG2 marker (green) and anti-6-His (red) to visualize AAV-mediated delivery of NG2Ab in the vicinity of NG2-positive processes. Merged images represent colocalization of anti-6-His with CC1, NeuN, ED-1, and NG2 signals, indicating AAV-NG2Ab-mediated transduction of oligodendrocytes, neurons, macrophages/microglia, and NG2-positive processes, respectively.

period, one subgroup of animals was also used for cystometry (see Materials and Methods).

In metabolic chamber experiments, we have compared parameters, such as total number of voids, intermicturition intervals, and volume per void. Consistent with previous research (LaPallo et al., 2017), voids were typically larger and less frequent in SCI animals (Fig. 4*A–C*). The results demonstrate that at week 6 after injury and treatment administration, rats from both treatment groups (AAV-NG2Ab and AAV-NG2AB+AAV-NT3) demonstrated significant recovery of bladder activity. Improvements were evident in increased number of voids, smaller mass per void and decreased time between voids. Number of voids was significantly higher in AAV-NG2Ab and AAV-NG2Ab+AAVNT3 groups compared with control AAV-GFP group. Number of voids was 36 ± 8 for AAV-NG2AB+AAV-NT3 group ($n = 8$), 24.8 ± 5 for AAV-NG2Ab group ($n = 8$), and only 10.5 ± 1.7 for group AAV-GFP ($n = 8$), 44.25 ± 5.79 (44.25 ± 5.79 for noninjured naive group; Fig. 4, $p < 0.05$). Evaluation of intermicturition intervals demonstrated similar recovery. Treated rats from AAV-NG2Ab and AAV-NG2AB+AAV-NT3 groups exhibited significantly shorter time between voids compared with control AAV-GFP group. Mean intermicturition interval was 26.9 ± 5.3 min for AAV-NG2AB+AAV-NT3 group, 40.2 ± 12 min for AAV-NG2Ab group, and 86.6 ± 12 min for AAV-GFP group (34.1 ± 8.19 for noninjured naive group; Fig. 4, $p < 0.05$). The data for average volume per void also showed better recovery in treated rats. The results demonstrate significantly smaller volume per void in rats from treatment group AAV-NG2AB+AAV-NT3 and AAV-NG2Ab compared with control AAV-GFP group. The mean volume per void was 0.18 ± 0.02 g for AAV-NG2AB+AAV-NT3 group; 0.41 ± 0.06 g for AAV-NG2Ab group and 0.53 ± 0.12 g for AAV-GFP group (0.25 ± 0.05 for noninjured naive group; Fig. 4, $p < 0.05$). Importantly, rats treated with AAV-NG2Ab+AAV-NT3 demonstrated significantly better bladder function compared with not only control group but also to rats treated with AAV-NG2Ab only as is

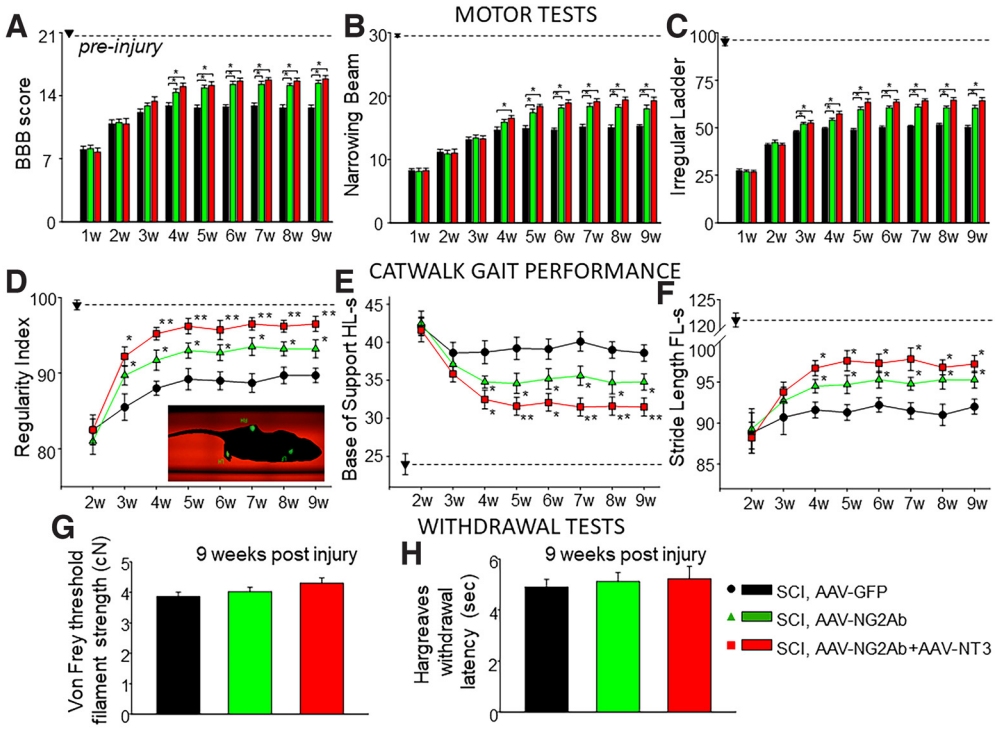

Figure 3. Treatment with AAV-NG2Ab and AAV-NT3 improved locomotor function after contusion SCI assessed by BBB, Narrowing Beam, Irregular Ladder, and CatWalk gait analysis. ***A–F***, Summary of results demonstrating significantly better locomotor performance evident in (***A***) BBB score, (***B***) longer distance passed in Narrowing Beam, (***C***) fewer number of slips in Irregular Ladder, (***D***) higher regularity index, (***E***) smaller base of support, and (***F***) longer stride length. Dotted line indicates pre-injury scoring for each motor test. Data are mean ± SEM ($n = 12$ rats per group). Pre-injury scoring for each motor test is indicated with the dotted line; data presented as mean ± SEM ($n = 12$ rats per group). *$p < 0.05$ statistical difference between control (AAV-GFP) group and treatment (AAV-NG2Ab alone, or AAV-NG2Ab + AAV-NT3) groups; **$p < 0.05$ statistical difference between AAV-NG2Ab alone and AAV-NG2Ab + AAV-NT3 groups (***D***, ***E***). Withdrawal reflex, measured as (***G***) von Frey threshold filament strength and (***H***) Hargreaves withdrawal latency, was not significantly affected by these treatments.

evident in intermicturition time and in volume per void ($p < 0.05$, Fig. 4*B*,*C*).

Cystometry

One subgroup of animals from all groups was used for terminal cystometry recordings to assess bladder function as previously described (D'Amico et al., 2011). Consistent with the results described above, cystometry experiments demonstrated improvements in bladder function, specifically evident in reduced number of nonvoiding contractions. Number of nonvoiding contractions is significantly increased in injured spinal cord and represents one of the main functional shortfalls after spinal cord injuries (Kim et al., 2006; Ward et al., 2014). Figure 4*D* shows examples of cystometry recordings conducted from a noninjured, AAV-GFP-injected rat and from a rat injected with AAV-NG2Ab and AAV-NT3. For each animal, we have compared the percentage of nonvoiding contractions out of total number of contractions during the recorded period (asterisks indicate nonvoiding contractions, Fig. 4*D*). For rats from the AAV-NG2AB+AAV-NT3 group, the percentage of nonvoiding contractions out of total number of contractions was 34 ± 17% ($n = 5$); for rats from the AAV-NG2Ab group, the percentage was 85 ± 26% ($n = 5$) and for rats from control AAV-GFP group the percentage was 136 ± 34% ($n = 5$). Results from terminal cystometry experiments revealed significantly reduced number of nonvoiding contractions in rats from AAV-NG2AB+AAV-NT3 group compared with control AAV-GFP-treated animals ($p < 0.05$; Fig. 4*E*).

In order to examine whether the functional changes observed were a result of administered treatments, we have also assessed the correlation between the spared tissue at the injury epicenter and changes in voiding for each animal (Fig. 4*F*). For each study group, we analyzed and compared the spared tissue between the groups. The mean spared tissue for the AAV-GFP group was 41.6 ± 1.0%, the AAV-NG2-Ab group was 42.6 ± 1.8%, and for the AAV-NG2-Ab+NT3 group was 42.2 ± 1.4% with no significant difference between the groups ($p > 0.05$). Correlation analysis revealed an absence of correlation (Fig. 4*F*) between the percentage of spared tissue area at the injury epicenter and ratio of nonvoiding contractions versus voiding as reported in Figure 4*E*. For the AAV-GFP group, AAV-NG2-Ab group, and AAV-NG2-Ab +NT3 group, correlation coefficients were $r = -0.10$ ($p = 0.849$), $r = -0.23$ ($p = 0.699$), and $r = -0.14$ ($p = 0.812$), respectively, using Pearson's correlation test (Fig. 4*F*). We have also analyzed and performed correlation analysis for the combined data from all groups between spared tissue and nonvoiding contractions (Fig. 4*F*, dotted line). Correlation analysis revealed no correlation between spared tissue and nonvoiding contraction across all groups ($r = -0.16$, $p = 0.54$). Thus, these results provide additional evidence that improved bladder function in animals from treatment groups was determined by the treatments that the rats received.

Treatment with AAV-NG2Ab and AAV-NT3 improved anatomic plasticity

We have further examined whether improved function after SCI and AAV-NG2Ab/AAV-NT3 treatment could be associated with improved anatomic plasticity. To visualize fibers that may form stronger or novel projections, we have examined (1) BDA anatomically traced fibers from SMC and (2) 5-HT immunoreactivity in lumbar gray matter.

BDA tracing

After completion of behavioral and metabolic chamber testing, one subgroup of animals from each group was dedicated to

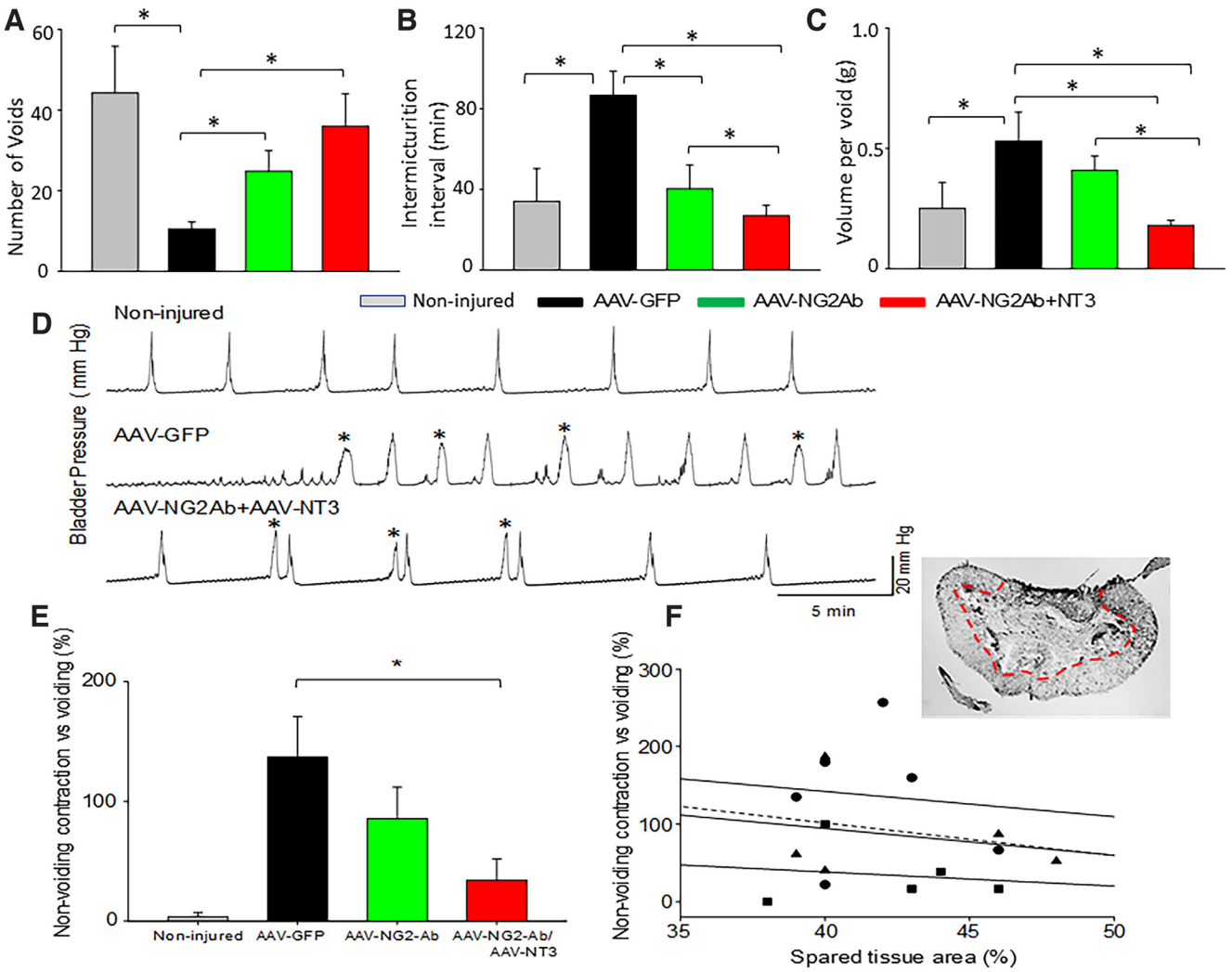

Figure 4. Treatment with AAV-NG2Ab and AAV-NT3 improved bladder function after contusion SCI. ***A–C***, Bladder function was assessed during the survival period using metabolic chambers to collect and quantify overnight urine production. Summary of results demonstrating improved bladder function evident in significant (***A***) increased number of voids, (***B***) decreased intermicturition intervals, and (***C***) decreased volume per void in treated rats compared with rats that received control treatment ($n = 8$ rats per group). ***D***, ***E***, Terminal cystometry electrophysiology recordings performed after 6 weeks after injury, with simultaneous acquisition of EUS EMG activity. ***D***, Representative traces of bladder pressure recordings demonstrating less nonvoiding contractions (asterisks) in treated rats compared with control treated rats. ***E***, Summary of results demonstrating significantly decreased number of nonvoiding contractions, in AAV-NG2Ab- and AAV-NT3-treated rats compared with control treated animals ($n = 5$ randomly selected rats per group). ***F***, Correlation between the spared tissue at the injury epicenter (outlined by dotted line on the image of the cryosection) and changes in voiding between groups (circles represent AAV-GFP; triangles represent AAV-NG2Ab; squares represent AAV-NG2Ab + AAV-NT3); analysis revealed an absence of correlation. Dotted line indicates correlation analysis for the combined data from all groups between spared tissue and nonvoiding contractions. Data are mean ± SEM. *$p < 0.05$.

examine how treatment with AAV-NG2Ab and AAV-NT3 effects anatomic plasticity. In particular, we have examined sprouting of corticospinal axons at cervical level (Fig. 5). Following bilateral injections of BDA tracer into the SMC, corticospinal axons were visualized using immunofluorescence staining (see Materials and Methods). BDA-labeled axons were analyzed in the gray matter of cervical segments C4-C5 to quantify and compare anatomic plasticity across treatment groups.

Representative images from AAV-GFP-injected group and AAV-NG2Ab+AAV-NT3-injected group are shown in Figure 5*A*, *B* and depict characteristic BDA labeling and gray mater anatomic area used for analysis. Our results revealed markedly more BDA-labeled fibers in AAV-NG2Ab+AAV-NT3 group compared with the AAV-GFP-treated group. Analysis showed significantly larger BDA-positive area in the cervical gray matter of AAV-NG2Ab+AAV-NT3 group 53.7 ± 3.0 ($n = 4$), compared with 44.6 ± 2.8 ($n = 4$) for AAV-GFP group ($p < 0.05$, Fig. 5*C*). AAV-NG2Ab-treated group did not show significant difference in BDA-positive area; 49.8 ± 2.1 ($n = 4$) ($p > 0.05$, Fig. 5*C*).

5-HT fibers

Serotonergic neurons possess an enhanced ability to regenerate or sprout after many types of injury (Holmes et al., 2005; Kim et al., 2006; Hawthorne et al., 2011). Previous studies have reported the effects of the degradation of proteoglycans with ChABC on recovery of 5-HT immunoreactivity (Tom et al., 2009; Alilain et al., 2011). Locomotor function recovery in rodents following spinal cord injuries correlates closely with recovery of 5-HT immunoreactivity (Saruhashi et al., 1996; Kim et al., 2006). In our previous study, we have demonstrated the effect of neutralization of NG2, using short-term delivery of monoclonal antibodies, on sprouting of 5-HT fibers after hemisection spinal cord injuries (Petrosyan et al., 2013). In the current study, we have examined how prolonged delivery of NG2 neutralization and neurotrophic support effects regeneration and sprouting of 5-HT fibers. We

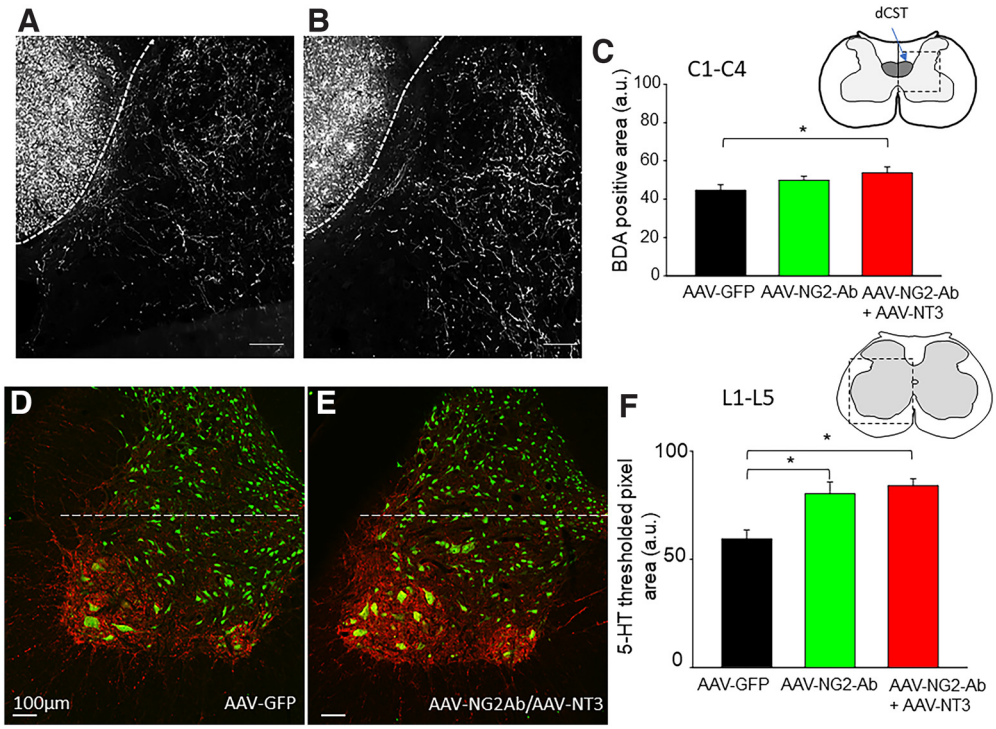

Figure 5. Treatment with AAV-NG2-Ab and AAV-NT3 following thoracic contusion promotes anatomic plasticity in damaged spinal cord. Treatment resulted in sprouting of corticospinal tract fibers in cervical spinal cord (***A–C***) and plasticity of serotonergic fibers in lumbar spinal cord (***D–F***). ***A***, ***B***, Representative images of BDA-labeled corticospinal tract fibers of animals from AAV-GFP control group and AAV-NG2-Ab + AAV-NT3 group, respectively. ***C***, Summary of results demonstrating significantly larger BDA-positive area in gray matter of AAV-NG2AB + AAV-NT3 group in C1-C4 levels compared with AAV-GFP or AAV-NG2Ab only groups. ***D***, ***E***, Representative images of 5-HT (red, to identify 5-HT-positive fibers) and Neu-N (green, to identify neurons) immunoreactivity in L5 segment (corresponding to position of recording electrodes in electrophysiology experiments) in animals from AAV-GFP control group and AAV-NG2-Ab + AAV-NT3 group, respectively. ***F***, Summary of quantitative analyses of thresholded pixel area of 5-HT-positive fibers revealed a significant increase in 5-HT-positive fibers in intermedial and ventral (outlined by dotted line) gray matter of AAV-NG2Ab and AAV-NG2AB + AAV-NT3 group in L1-L5 levels. Data are mean ± SEM ($n = 5$ rats/group). *$p < 0.05$.

measured 5-HT immunoreactivity as thresholded pixel area, as described previously (Tom et al., 2009; Hunanyan et al., 2013; Petrosyan et al., 2013). We have quantified 5-HT immunoreactivity in L1-L5 segments in all three experimental groups. Figure 5 demonstrates representative images taken from sections from the control AAV-GFP group (Fig. 5*D*) and the AAV-NG2 and AAV-NT3-treated group (Fig. 5*E*), demonstrating typical 5-HT signal and area of analysis (intermediate and ventral gray matter) outlined by the dotted line. Our results demonstrate that there is significantly higher 5-HT immunoreactivity in lumbar segments in both treatment groups. Both treatment groups (i.e., AAV-NG2Ab and AAV-NG2AB+AAV-NT3) showed higher 5-HT immunoreactivity in intermediate and ventral gray matter in L1-L5 segments (Fig. 5*F*). Area of 5-HT-positive immunoreactivity in L1-L5 segments of group treated with AAV-GFP was 59.3 ± 4.1, group treated with AAV-NG2Ab was 80.2 ± 5.4, and group treated with AAV-NG2Ab+AAV-NT3 was 84 ± 3.2 (Fig. 5*F*, $n = 5$ rats per group, $p < 0.05$).

Treatment with AAV-NG2Ab and AAV-NT3 improved transmission

One subgroup of animals from each group was dedicated for *in vivo* terminal electrophysiological evaluation of transmission to lumbar spinal cord from segments rostral to injury. Intracellular and extracellular responses were recorded from the L5 ventral horn motoneurons pool in response to electric stimulation of LWM tracts at the T6 spinal level. Consistent with the results of behavioral experiments and bladder evaluation, animals from treatment groups, AAV-NG2Ab and AAV-NG2Ab+AAVNT3, showed markedly increased amplitude of intracellular responses recorded from L5 ventral horn motoneurons compared with the group treated with AAV-GFP only (Fig. 6*A*). At weeks 9-12 after injury and treatment administration, mean amplitude of intracellular responses recorded from animals of control SCI group; that is, AAV-GFP was 0.81 ± 0.14 mV ($n = 6$). Mean amplitude recorded from animals from the group treated with AAV-NG2Ab was 1.82 ± 0.27 mV ($n = 6$) and was significantly larger compared with responses recorded from control animals ($p < 0.05$; Fig. 6*A2*). Animals from the group treated with both treatments, combination of AAV-NG2Ab and AAV-NT3, showed the best improvements in synaptic transmission (Fig. 6*A*). The mean amplitude of intracellular responses recorded from these rats was 3.03 ± 0.39 mV ($n = 6$) and was significantly larger compared with control animals ($p < 0.05$; Fig. 6*A2*).

We have recently reported improvements of transmission and motor function following an identical T10 contusion protocol in rats treated with intraspinal injections of ChABC combined with AAV-NT-3 (Hunanyan et al., 2013). Since in the current study the same injury model and recording technique were used as in our previous study (Hunanyan et al., 2013), we have compared results from that study with our current results. Comparisons of the results revealed that intraspinal injections of AAV-NG2Ab combined with AAV-NT3 after contusion SCI induced better improvement of synaptic transmission than administration of ChABC combined with AAV-NT3 in the identical SCI model. These results provide additional evidence emphasizing the importance of prolonged neutralization of NG2 proteoglycan after SCI.

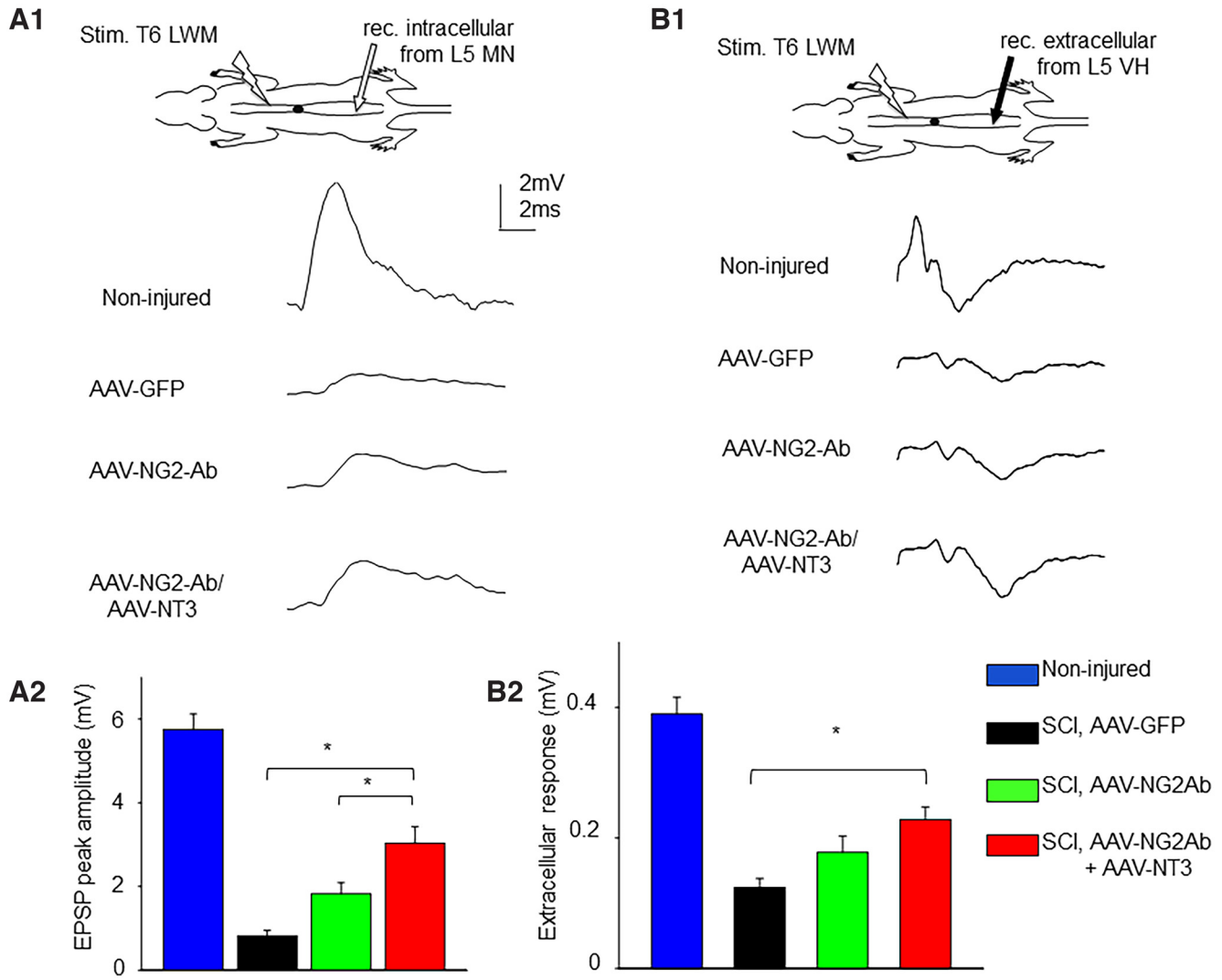

Figure 6. AAV-NG2Ab combined with AAV-NT3 improved transmission to lumbar motoneurons in chronically contused rats. ***A***, ***B***, Representative traces of intracellular (***A1***) and extracellular (***B1***) responses (10 averaged consecutive responses) recorded from L5 ventral horn and evoked by electric stimulation of LWM at T6 demonstrating larger amplitude in rats from AAV-NG2Ab group and AAV-NG2AB+AAV-NT3 group compared with control treated rats. ***A2***, Summary of results demonstrating significant facilitation of intracellular responses recorded from L5 ventral horn neurons in AAV-NG2Ab-treated and AAV-NG2Ab+AAV-NT-3-treated rats compared with control AAV-GFP-treated rats. ***B2***, Summary of results demonstrating similar significant facilitation of extracellular responses in AAV-NG2Ab-treated and AAV-NG2Ab+AAV-NT-3-treated rats compared with control AAV-GFP-treated rats. Diagram represents position of stimulation and recording electrodes. Data are mean ± SEM. *$p < 0.05$. In the same graph (***A2***), we have compared effects of AAV-NG2Ab and AAV-NT3 on transmission with the results of our previous study where we have examined the effects of intraspinal injections of ChABC (adopted from Hunanyan et al., 2013).

We have also recorded and compared responses recorded extracellularly from lumbar spinal cord for these animals (Fig. 6*B1*). Results of extracellular recordings revealed that, in accordance with intracellular experiments, similar improvements of transmission were observed in treated rats. Mean amplitude for animals treated with AAV-GFP was 0.12 ± 0.01 mV ($n = 6$), for animals treated with AAV-NG2Ab only was 0.17 ± 0.02 mV ($n = 6$), and for animals treated with AAV-NG2AB+AAV-NT3 was 0.22 ± 0.01 mV ($n = 6$). Mean amplitude of extracellular responses recorded from L5 spinal cord was significantly higher in AAV-NG2AB+AAV-NT3 treatment group versus AAV-GFP control group ($p < 0.05$, Fig. 6*B2*).

Axonal excitability

To examine possible effects of neutralization of NG2 proteoglycan on the physiological functions of the spared axons and to better understand mechanisms underlying the improved synaptic transmission in lumbar spinal cord, we conducted intra-axonal recordings from individual axons in L1 white matter as previously described (Hunanyan et al., 2011; Petrosyan et al., 2013). By applying both hyperpolarizing and depolarizing current steps through the recording microelectrode, we were able to measure membrane potential and examined membrane properties for each axon that was possible to record. We have determined the rheobase of axons (i.e., the minimum depolarization current required to induce AP) (Hunanyan et al., 2011; Petrosyan et al., 2013).

We have found that, consistent with results reported above, treatment with AAV-NG2Ab and AAV-NT3 decreased the rheobase of axons compared with control rats (Fig. 7). Rats from group treated with AAV-NG2Ab and from group treated with AAV-NG2AB+AAV-NT3 exhibited increased excitability of axons compared with control group treated with AAV-GFP only; mean rheobase current for AAV-GFP group was 0.74 ± 0.03 nA ($n = 4$, 24 axons), for AAV-NG2Ab-treated group was 0.65 ± 0.03 nA ($n = 4$, 26 axons), and for group treated with AAV-NG2Ab+AAV-

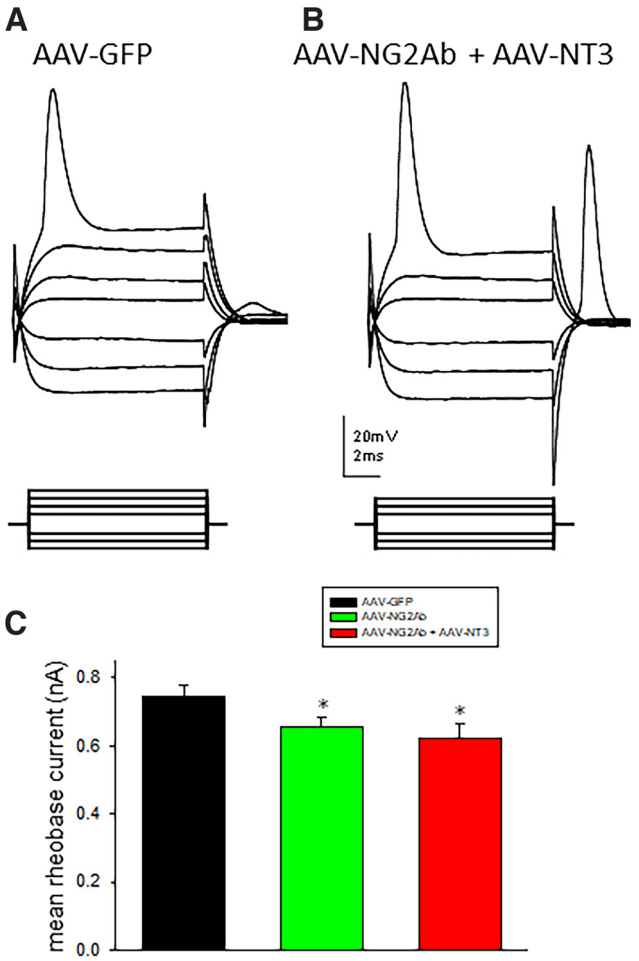

Figure 7. AAV-NG2Ab combined with AAV-NT3 treatment improved axonal excitability. ***A***, ***B***, Representative traces of intra-axonal recording performed from individual axons in L1-L2 LWM, recorded from AAV-GFP-anesthetized (***A***) and AAV-NG2AB+AAV-NT3-anesthetized (***B***) rats, respectively, demonstrating increased excitability (lower rheobase current) and absence of changes in the input resistance of axons in rats from AAV-NG2AB+AAV-NT3 group compared with control contused treated with AAV-GFP group rats. ***C***, Summary of results demonstrating significantly lower rheobase current in both AAV-NG2Ab ($n = 26$ axons) and AAV-NG2AB+AAV-NT3 ($n = 22$ axons) groups compared with AAV-GFP group ($n = 24$ axons). Data are mean ± SEM. *$p < 0.05$.

NT3 was 0.62 ± 0.04 nA ($n = 4$, 22 axons) ($p < 0.05$; Fig. 7). The mean input resistance of the axons acquired through hyperpolarizing current pulses was not significantly different (Fig. 7). These results demonstrate that treatment groups demonstrate the state of spared axons are improved (i.e., excitability of individual axons is increased), which is known to be diminished in injured spinal cord (Hunanyan et al., 2011). The termination of the hyperpolarizing current (anode break) triggered an AP with an increased amplitude in many axons recorded from cords of SCI animals treated with AAV-NG2Ab+AAV-NT3 (in 35 of 51 axons recorded, Fig. 7*B*). This is consistent with properties of APs recorded *in vitro* from lumbosacral axons (Kocsis and Waxman, 1982) and dorsal root axons (Novak et al., 2009) in rats. However, fewer axons in SCI AAV-GFP-treated animals (11 of 47 axons recorded) showed an anode break excitation after termination of the hyperpolarizing current. Interestingly, our previous study revealed that the generation of the AP as an anode break excitation after termination of the hyperpolarizing current has often been seen in axons of noninjured animals, but rarely in axons of chronic SCI animals (Hunanyan et al., 2011). These results suggest that, in certain cases, treatment with AAV-NG2Ab+AAV-NT3 shifts electrophysiological properties of individual axons toward properties of axons seen in noninjured animals. Cellular mechanisms of this phenomenon have not been determined.

Relation of NG2-positive processes with nodes of Ranvier

We have recently discovered that, consistent with new inhibitory function of NG2 (i.e., blocking of axonal conduction and transmission to motoneurons) (Hunanyan et al., 2010), many NG2-positive processes contact nodes of Ranvier within the nodal gap at the location of nodal Na channels (Petrosyan et al., 2013), which are known to be directly involved in propagation of APs along spinal axons (Wang et al., 1997; Black et al., 2006). Insertion of NG2 cell processes at the nodes has been recently confirmed by another group (Serwanski et al., 2017). Importantly, we recently found that the number of nodes that make close contacts with NG2 processes was significantly higher in SCI versus naive animals (Petrosyan et al., 2013).

In this study, we have examined whether improvements in synaptic transmission (Fig. 6) and axonal excitability (Fig. 7) in treatment groups are associated with changes of the anatomic relationship of NG2-positive processes and nodes of Ranvier. We have performed double immunostaining with NG2 and CASPR to visualize NG2-positive processes in relation to the nodes of Ranvier in AAV-GFP, AAV-NG2Ab, and AAV-NG2AB+AAV-NT3 groups (Fig. 8*A–C*). Using horizontal sections from spinal T9-T11 levels, we have examined the number of nodes of Ranvier containing NG2-positive processes (Fig. 8*A*,*B*). In each section, we have quantified the percentage of nodes containing NG2-positive processes out of total number of nodes in that section. The results revealed no significant difference between the groups in the number of nodes containing NG2-positive processes (Fig. 8*C*). The percentage of nodes containing NG2-positive processes out of total number of nodes counted in control group treated with AAV-GFP was 15.7 ± 0.86, AAV-NG2Ab-treated group showed 14.7 ± 0.8, and AAV-NG2AB+AAV-NT3-treated group showed 18.7 ± 1.9. These results suggest that treatment with AAV-NG2Ab-induced changes of axonal excitability and synaptic transmission as reported in this study are not associated with changes in the presence of NG2-positive processes at the nodes of Ranvier (Fig. 8*A–C*). Comparison of high-power confocal images of the nodes did not demonstrate any obvious structural changes at the node of Ranvier in animals treated with AAV-GFP, AAV-NG2Ab, and AAV-NG2Ab+AAV-NT3.

Additionally, we used alternating longitudinal sections for double immunostaining with CASPR and 6-His, to examine AAV-mediated transduction with AAV-NG2Ab in relation to nodes of Ranvier (Fig. 8*D*,*E*). Results demonstrate that many AAV-NG2Ab-positive cells and processes have been visualized in close association with the nodes in AAV-NG2Ab-treated animals.

Another set of alternating longitudinal sections has been used for double immunostaining for NG2 and AAV-NG2Ab, to visualize the presence of AAV-NG2Ab in the vicinity of NG2-positive cells and processes along LWM axons caudal to contusion (Fig. 8*F*).

Overall, our results using immunohistochemistry and confocal imaging confirm presence of NG2-positive processes in close relation to the nodal gap (Fig. 8*A*,*B*), presence of many processes transduced with AAV-NG2Ab making close contact with the nodes of Ranvier (Fig. 8*D*,*E*), as well as presence of AAV-

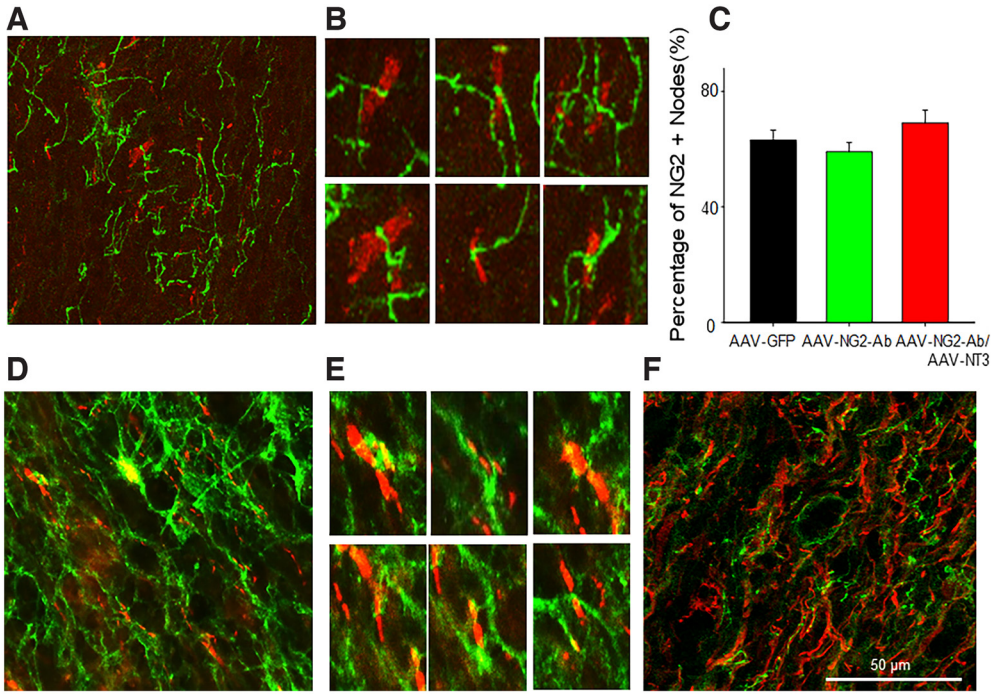

Figure 8. Horizontal section of T9-T11 spinal cord double-immunostained with CASPR and NG2 (***A***,***B***) and CASPR and 6-His for NG2-Ab (***D***,***E***) to demonstrate localization of NG2-positive processes and AAV-mediated delivery of NG2-Ab in relation to nodes of Ranvier, in the LWM caudal to injury at the depth corresponding to VLF. High-power confocal images selected from the low-power image (***B***) represent (***A***) individual nodes (red) and NG2-positive processes (green). ***C***, Summary of results demonstrating no significant difference in the percentage of nodes containing NG2-positive processes between groups. ***D***, ***E***, Alternating longitudinal sections representing double immunostaining with CASP (red) and 6-His (green). Low- and high-power confocal images, respectively, demonstrate colocalization of AAV-NG2Ab-positive processes (green) in close association with the nodes (red). ***F***, Images from alternating sections: double immunostaining of NG2 (green) and AAV-mediated delivery of NG2-Ab (red; 6-HIS traced), along LWM axons caudal to contusion. Data are mean ± SEM.

NG2Ab in the vicinity of NG2-positive processes (Fig. 8*F*). Our results using immunohistochemistry and confocal imaging, however, did not demonstrate any obvious structural changes at the node of Ranvier or change in percentage of nodes containing NG2-positive processes between groups (Fig. 8*A–C*). These results suggest that AAV-NG2Ab attenuates the effect of NG2 on axonal conduction without physically removing NG2 processes from nodes of Ranvier.

Effects of treatment with AAV-NG2Ab and AAV-NT3 on myelination

Current results demonstrating improved transmission in spinal cord (Fig. 6) and in particular improved excitability of single axons (Fig. 7) prompted us to determine whether treatment with AAV-NG2Ab improved myelination of spared spinal cord axons after contusion SCI. Since demyelination of axons after contusion SCI in addition to injury epicenter progresses gradually to white matter tracts several millimeters caudal and rostral to injury epicenter (Siegenthaler et al., 2007), we have investigated myelin structures in L1 spinal cord white matter fibers. We have performed immunohistochemistry experiments on longitudinal section to visualize MBP, as well as electron microscopy experiments on transverse sections to determine the thickness of myelin sheets of axons and calculated the G-ratio of these axons.

Our experiments with MBP staining demonstrate significantly higher MBP-staining signal in the spinal cord of rats treated with AAV-NG2Ab+AAV-NT3 compared with AAV-NG2Ab-treated or AAV-GFP-treated rats (Fig. 9*A*,*B*). Mean MBP signal in AAV-NG2Ab+AAV-NT3-treated rats was 110 ± 4.2, in AAV-NG2Ab-treated rats was 95 ± 2.5, and AAV-GFP-treated rats exhibit 93 ± 4.2, respectively ($n = 5$ rats per group, $p < 0.05$, Fig. 9*C*). Further, we have performed electron microscope experiments to quantitively examine the number of myelinated axons and the thickness of myelin sheets of axons in LWM. Electron microscopy experiments revealed no significant difference in G-ratio of myelinated axons between experimental groups ($p > 0.05$, Fig. 9*D–F*). Analysis of G-ratio for mixed population (large and small diameter) of myelinated axons revealed that AAV-GFP-treated rats exhibit 33.9 ± 2.8 ($n = 5$), AAV-NG2Ab-treated rats 32.8 ± 2.2 ($n = 5$), and AAV-NG2Ab+AAV-NT3 33.5 ± 2.6 ($n = 5$), respectively ($p > 0.05$, Fig. 9*F*). However, the percentage of myelinated fibers, calculated as a percent of the total quantified number of axons, revealed a significantly higher number of myelinated axons in AAV-NG2AB+AAV-NT3-treated rats compared with the other two groups ($p < 0.05$, Fig. 9*G*). Animals from AAV-NG2Ab+AAV-NT3 revealed 41.5 ± 2.34% ($n = 5$) versus AAV-GFP-treated group 34.1 ± 1.58% ($n = 5$; $p < 0.05$) and versus AAV-NG2Ab-treated rats 36.5 ± 2.41% ($n = 5$; $p < 0.05$), respectively. These results are in accordance with immunohistochemical experiments demonstrating higher MBP signal in AAV-NG2Ab+AAV-NT3-treated versus control or AAV-NG2Ab-treated rats (Fig. 9*C*).

Discussion

In this study, we demonstrate the beneficial effects of AAV-mediated transduction with NG2Ab for neutralization of inhibitory function of NG2 proteoglycan, combined with AAV-mediated transduction with neurotrophin NT3, on the recovery of function after contusion SCI. Best improvements of both locomotor (Fig. 3) and bladder (Fig. 4) functions were seen in the group that received combined AAV-NG2Ab and AAV-NT3 treatments. These beneficial

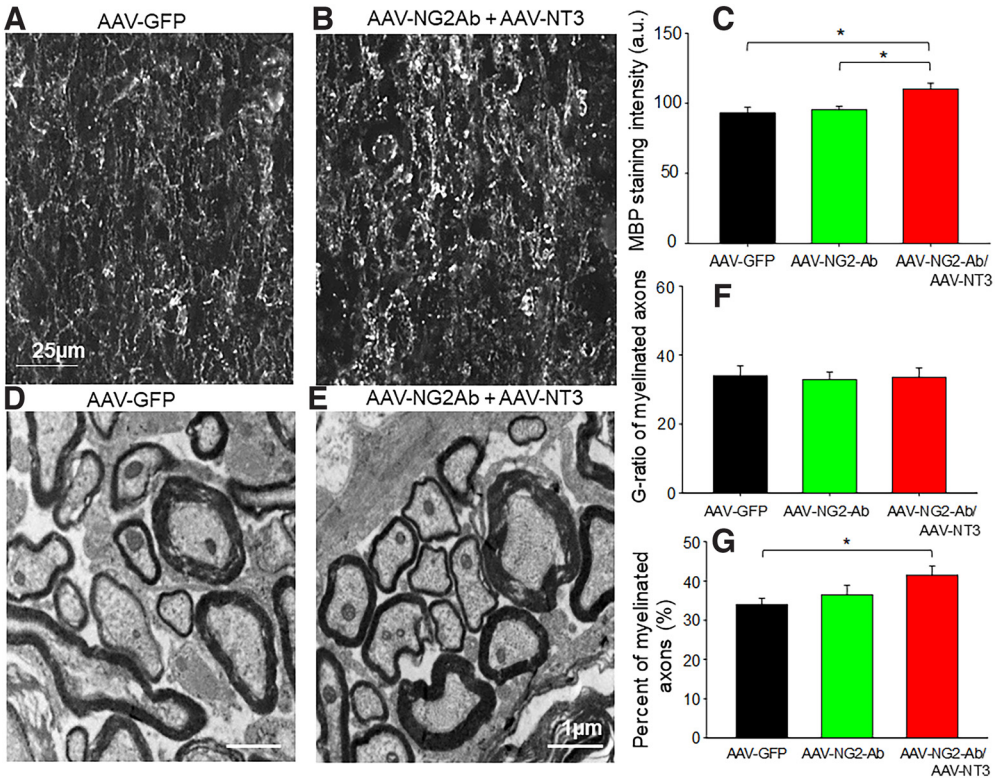

Figure 9. Effects of treatment with AAV-NG2Ab and AAV-NT3 on myelination in chronically injured rats. ***A***, ***B***, Representative images of spinal cord sections immunostained with MBP taken from AAV-GFP-treated (***A***) and AAV-NG2AB+AAV-NT3-treated (***B***) animals, respectively. ***C***, Summary of results demonstrating significantly higher MBP staining in AAV-NG2Ab+AAV-NT3-treated animals compared with AAV-NG2Ab only and AAV-GFP groups. ***D***, ***E***, Representative electron microscope images of spinal cords from AAV-GFP-treated (***D***) and AAV-NG2Ab+AAV-NT3-treated (***E***) rats, respectively. ***F***, Summary of results demonstrating no significant difference in G-ratio of fibers between groups. ***G***, Summary of results demonstrating significantly higher percentage of myelinated axons in AAV-NG2AB+AAV-NT3-treated rats compared with other groups. Data are mean ± SEM. *$p < 0.05$.

effects of combined treatment on recovery of function after SCI associated with (1) improved anatomic plasticity in damaged spinal cord (i.e., sprouting of BDA-labeled corticospinal tract fibers in cervical spinal cord) and an increase in 5-HT-positive fibers in intermedial and ventral gray matter in lumbar cord (Fig. 5), (2) improved synaptic transmission to lumbar motoneurons (Fig. 6), (3) improved reobase, and thus partially recovered excitability of axons in the LWM in damaged spinal cord (Fig. 7), and (4) significantly higher percentage of myelinated axons (Fig. 9).

Why AAV-rh10?

In this study, we used AAV-rh10 vector for transgene delivery of NG2-Ab and NT-3. The choice of this specific serotype of AAV was based on our previous observations demonstrating that, although the efficacy to transduce neurons was comparable to established AAV-1, -5, and -9 serotypes, AAV-rh10 transduced significantly higher numbers of macrophages/microglia and oligodendrocytes in the damaged spinal cord (Petrosyan et al., 2014). The role of both macrophages/microglia and oligodendrocytes in secondary damage following SCI and recovery cannot be underestimated and has been widely reported (Zhou et al., 2020). The recent reports confirmed that, among the various serotypes tested, AAVrh10 displayed favorable tropism for neurons, astrocytes, and oligodendrocytes with the large expression in the injury epicenter and extention into the surrounding tissue (Hoshino et al., 2019). The excellent trophism to neurons and glial cells urged us to use AAV-rh10 as a tool for transgene delivery of NG2 function neutralizing antibody and NT3 to injured spinal cord (Figs. 1, 2).

AAV10-NT3

Neurotrophins' neuroprotective function and the ability to promote remyelination, sprouting, and growth of axons in the damaged spinal cord highlight their importance for regenerative repairs after SCI (for review, see Tuszynski and Gage, 1995; Bregman et al., 2002; Bunge and Pearse, 2003; Murray et al., 2004; de Groat and Yoshimura, 2006; Arvanian, 2013). The AAV-mediated transgene delivery of neurotrophins has been recognized as an effective treatment for SCI (Blits et al., 2003; Boyce et al., 2012). It was shown to partially reverse chronic pain after SCI (Eaton et al., 2002), rescue atrophy of rubrospinal neurons (Ruitenberg et al., 2004), and motoneurons (Blits et al., 2003), but induced only modest improvement of locomotor function in SCI models (Fortun et al., 2009; Williams et al., 2012). Our previous results suggest that AAV-mediated transgene delivery of NT3 is an important component of combination treatment, but not AAV-NT3 administered alone (Hunanyan et al., 2013; Petrosyan et al., 2015).

SCPGs and synaptic transmission in damaged spinal cord

Our previous studies revealed that, after thoracic T10 contusion, the disrupted dorsal corticospinal tract axons spontaneously form new synaptic contacts with individual motoneurons, extending around the contusion cavity, through spared VLF (Hunanyan et al., 2013). Strengthening of these weak detour connections to improve function may be a target for therapeutic interventions after SCI. Decline of synaptic transmission in damaged spinal cord at 2 weeks after injury coincided with the arrest of behavioral recovery (García-Alías et al., 2011); and the time

when the elevated level of CSPGs, particularly NG2, in tissue surrounding the injury epicenter was maximum (Snow et al., 1990; McKeon et al., 1991; Davies et al.,1997; Silver and Miller, 2004; Galtrey and Fawcett, 2007). Digestion of CSPGs, although found to improve axonal sprouting, induced little or no recovery of function following SCI; better improvements were seen when ChABC was combined with neurotrophins (Massey et al., 2008; Tom et al., 2009; Lee et al., 2010; Hunanyan et al., 2013).

SCPGs are part of extracellular matrix that supports neuronal and glial cells. The abnormal deposition of CSPGs at the injury site is detrimental to regeneration since many, but not all, CSPGs have been reported to mediate axon growth inhibition (Gaudet and Popovich, 2014). Because of the diverse properties of CSPGs, it may be more beneficial to neutralize a single CSPG or a family of CSPGs rather than degrading all CSPGs (Zhou et al., 2001; Brakebusch et al., 2002; Bartus et al., 2014). Results of the current study provide additional evidence supporting the suggestion that neutralization of inhibitory function of a single proteoglycan NG2 can induce significant changes of transmission in spared fibers and thus have beneficial effect on the recovery of locomotor and bladder functions after SCI.

Role of NG2 and effects of AAV-NG2Ab

NG2 is a unique transmembrane-type CSPG, with a core protein containing the large ectodomain comprised of an N-terminal globular (Domain 1), a central extended domain that has the sites for GAG attachment (Domain 2) and a juxtamembrane domain (Domain 3) (Stallcup, 2002; Ughrin et al., 2003). NG2 expression occurs mainly in OPCs, and its level was found to be abnormally elevated in the vicinity of the injury. The physiological role of NG2 itself, however, has not been clearly understood.

Several reports suggest that accumulation of NG2 exerts an inhibitory effect on axonal growth: NG2 was found to inhibit neurite growth, treatment with ChABC partially neutralized the inhibitory nature of NG2 on neurite growth (Ughrin et al., 2003; Kilcoyne et al., 2012); the core protein of NG2 was demonstrated to contribute to the inhibition of neurite growth as well (Dou and Levine, 1994; Yiu and He, 2006). Inhibitory effects of NG2 on axonal growth in SCI have been overcome by administration of monoclonal antibody specifically against Domain 1 of NG2 (Tan et al., 2006).

Other reports, however, suggest the importance of NG2 molecule in several CNS functions. One recent study has demonstrated the important physiological role of the NG2 protein in the function of synapses: the lack of NG2 expression in OPCs in NG2 KO mice resulted in significant impairment of NMDA-dependent long-term facilitation in the SMC and administration of NG2 ectodomain reversed these functions (Sakry et al., 2014). Examination of NG2 KO mice for regeneration of the lesioned axons in another study revealed that in NG2 KO mice, sensory axons in the dorsal columns dieback further compared with WT (Filous et al., 2014). These studies using KO mice as a model indicate the importance of physical presence of NG2 molecule in various functions.

Since our recent electrophysiology experiments revealed new inhibitory function of NG2 to block axonal conduction (Hunanyan et al., 2010); and in an attempt to design an approach for safe, prolonged, and clinically feasible delivery of NG2-Ab, we have successfully created the new and unique gene therapy tool for delivery of a recombinant scFv anti-NG2 antibody: AAV-10 serotype expressing scFv-NG2 (AAV-NG2Ab).

Importantly, in our study, we use AAV-mediated delivery of monoclonal antibody designed to specifically bind and neutralize function of Domain 1 of NG2 proteoglycan, without interference with other domains of NG2. Our results demonstrating improvement of transmission to individual motoneurons (Fig. 6) and excitability of individual axons (Fig. 7) in damaged spinal cord strongly suggest that Domain 1 of NG2 is responsible for NG2-induced block of axonal conduction in addition to the earlier reported inhibitory role of this specific domain on axonal growth (Ughrin, 2003; Tan et al., 2006).

NG2 and nodes of Ranvier

Several studies have reported the presence of NG2-positive processes in the nodes of Ranvier (Butt et al., 1999; Serwanski et al., 2017). However, the exact role of glial processes at the nodes, especially from OPCs, are unknown. The presence of NG2-positive processes at the nodes may detect changes in myelination of the axons and trigger the differentiation of OPCs into myelinating cells when needed (Serwanski et al., 2017). Our previous results showed that, after SCI, the number of nodes with close contacts to NG2-positive processes are significantly higher compared with noninjured rats (Petrosyan et al., 2013), and this was hypothesized as a possible explanation for diminished conduction in damaged spinal cord. Results of the current study confirmed the presence of NG2-positive processes in close relation to the nodes (Fig. 8*A*,*B*) and detect the extensive presence of AAV-NG2Ab (identified by 6His tag) in close relation and inside of nodes of Ranvier (Fig. 8*E*).

Our results using immunohistochemistry and confocal imaging, however, did not demonstrate significant difference in the percentage of nodes containing NG2-positive processes between control SCI AAV-GFP and AAV-NG2Ab groups, or any obvious structural changes at the node of Ranvier (Fig. 8). These results suggest that the NG2-Ab may block the effect of NG2-positive processes on conduction without physically removing these processes from nodes of Ranvier. Further studies using electron microscopy are needed to demonstrate whether these physiological changes are associated with the position of NG2 processes within the node. Possible changes can include interaction of NG2 proteoglycan with sodium channels at the nodes, thus affecting its ability to block conduction.

References

Alilain WJ, Horn KP, Hu H, Dick TE, Silver J (2011) Functional regeneration of respiratory pathways after spinal cord injury. Nature 475:196–200.

Andrews EM, Richards RJ, Yin FQ, Viapiano MS, Jakeman LB (2012) Alterations in chondroitin sulfate proteoglycan expression occur both at and far from the site of spinal contusion injury. Exp Neurol 235:174–187.

Arvanian VL, Schnell L, Lou L, Golshani R, Hunanyan A, Ghosh A, Pearse DD, Robinson JK, Schwab ME, Fawcett JW, Mendell LM (2009) Chronic spinal hemisection in rats induces a progressive decline in transmission in uninjured fibers to motoneurons. Exp Neurol 216:471–480.

Arvanian V (2013) Role of neurotrophins in spinal plasticity and locomotion. Curr Pharm Des 19:4509–4516.

Arvanian VL, Petrosyan HA, Alessi A, Phagu N, Levine J, Collins WF (2016) Viral vector mediated neutralization of NG2 proteoglycan (AAV-NG2Ab) combined with delivery of neurotrophin NT-3 (AAV-NT3) improves transmission, locomotion and urinary tract function after incomplete spinal cord injury in adult rats. Soc Neurosci Abstract 612:

Bareyre FM, Kerschensteiner M, Raineteau O, Mettenleiter TC, Weinmann O, Schwab ME (2004) The injured spinal cord spontaneously forms a new intraspinal circuit in adult rats. Nat Neurosci 7:269–277.

Bartus K, James ND, Didangelos A, Bosch KD, Verhaagen J, Yáñez-Muñoz RJ, Rogers JH, Schneider BL, Muir EM, Bradbury EJ (2014) Large-scale chondroitin sulfate proteoglycan digestion with chondroitinase gene therapy leads to reduced pathology and modulates macrophage phenotype following spinal cord contusion injury. J Neurosci 34:4822–4836.

Basso DM, Beattie MS, Bresnahan JC (1996) Graded histological and locomotor outcomes after spinal cord contusion using the NYU weight-drop device versus transection. Exp Neurol 139:244–256.

Black JA, Waxman SG, Smith KJ (2006) Remyelination of dorsal column axons by endogenous Schwann cells restores the normal pattern of Na(v) 1.6 and K(v)1.2 at nodes of Ranvier. Brain 129:1319–1329.

Blits B, Oudega M, Boer GJ, Bartlett Bunge M, Verhaagen J (2003) Adeno-associated viral vector-mediated neurotrophin gene transfer in the injured adult rat spinal cord improves hind-limb function. Neuroscience 118:271–281.

Boyce VS, Park J, Gage FH, Mendell LM (2012) Differential effects of brain-derived neurotrophic factor and neurotrophin-3 on hindlimb function in paraplegic rats. Eur J Neurosci 35:221–232.

Brakebusch C, et al. (2002) Brevican-deficient mice display impaired hippocampal CA1 long-term potentiation but show no obvious deficits in learning and memory. Mol Cell Biol 22:7417–7427.

Bregman BS, Coumans JV, Dai HN, Kuhn PL, Lynskey J, McAtee M, Sandhu F (2002) Transplants and neurotrophic factors increase regeneration and recovery of function after spinal cord injury. Prog Brain Res 137:257–273.

Bunge MB, Pearse DD (2003) Transplantation strategies to promote repair of the injured spinal cord. J Rehabil Res Dev 40(4 Suppl 1):55–62.

Butt AM, Duncan A, Hornby MF, Kirvell SL, Hunter A, Levine JM, Berry M (1999) Cells expressing the NG2 antigen contact nodes of Ranvier in adult CNS white matter. Glia 26:84–91.

D'Amico SC, Collins WF 3rd (2012) External urethral sphincter motor unit recruitment patterns during micturition in the spinally intact and transected adult rat. J Neurophysiol 108:2554–2567.

D'Amico SC, Schuster IP, Collins WF 3rd (2011) Quantification of external urethral sphincter and bladder activity during micturition in the intact and spinally transected adult rat. Exp Neurol 228:59–68.

Davies SJ, Fitch MT, Memberg SP, Hall AK, Raisman G, Silver J (1997) Regeneration of adult axons in white matter tracts of the central nervous system. Nature 390:680–683.

de Groat WC, Yoshimura N (2006) Mechanisms underlying the recovery of lower urinary tract function following spinal cord injury. Prog Brain Res 152:59–84.

Dityatev A, Schachner M, Sonderegger P (2010) The dual role of the extracellular matrix in synaptic plasticity and homeostasis. Nat Rev Neurosci 11:735–746.

Dou CL, Levine JM (1994) Inhibition of neurite growth by the NG2 proteoglycan. J Neurosci 14:7616–7628.

Eaton MJ, Blits B, Ruitenberg MJ, Verhaagen J, Oudega M (2002) Amelioration of chronic neuropathic pain after partial nerve injury by adeno-associated viral (AAV) vector-mediated over-expression of BDNF in the rat spinal cord. Gene Ther 9:1387–1395.

Fidler PS, Schuette K, Asher RA, Dobbertin A, Thornton SR, Calle-Patino Y, Muir E, Levine JM, Geller HM, Rogers JH, Faissner A, Fawcett JW (1999) Comparing astrocytic cell lines that are inhibitory or permissive for axon growth: the major axon-inhibitory proteoglycan is NG2. J Neurosci 19:8778–8788.

Filous AR, Tran A, Howell CJ, Busch SA, Evans TA, Stallcup WB, Kang SH, Bergles DE, Lee SI, Levine JM, Silver J (2014) Entrapment via synaptic-like connections between NG2 proteoglycan^{+} cells and dystrophic axons in the lesion plays a role in regeneration failure after spinal cord injury. J Neurosci 34:16369–16384.

Fortun J, Puzis R, Pearse DD, Gage FH, Bunge MB (2009) Muscle injection of AAV-NT3 promotes anatomical reorganization of CST axons and improves behavioral outcome following SCI. J Neurotrauma 26:941–953.

Fouad K, Pedersen V, Schwab ME, Brösamle C (2001) Cervical sprouting of corticospinal fibers after thoracic spinal cord injury accompanies shifts in evoked motor responses. Curr Biol 11:1766–1770.

Galtrey CM, Fawcett JW (2007) The role of chondroitin sulfate proteoglycans in regeneration and plasticity in the central nervous system. Brain Res Rev 54:1–18.

García-Alías G, Petrosyan HA, Schnell L, Horner PJ, Bowers WJ, Mendell LM, Fawcett JW, Arvanian VL (2011) Chondroitinase ABC combined with neurotrophin NT-3 secretion and NR2D expression promotes axonal plasticity and functional recovery in rats with lateral hemisection of the spinal cord. J Neurosci 31:17788–17799.

Gaudet AD, Popovich PG (2014) Extracellular matrix regulation of inflammation in the healthy and injured spinal cord. Exp Neurol 258:24–34.

Hamers FP, Lankhorst AJ, van Laar TJ, Veldhuis WB, Gispen WH (2001) Automated quantitative gait analysis during overground locomotion in the rat: its application to spinal cord contusion and transection injuries. J Neurotrauma 18:187–201.

Hargreaves K, Dubner R, Brown F, Flores C, Joris J (1988) A new and sensitive method for measuring thermal nociception in cutaneous hyperalgesia. Pain 32:77–88.

Hawthorne AL, Hu H, Kundu B, Steinmetz MP, Wylie CJ, Deneris ES, Silver J (2011) The unusual response of serotonergic neurons after CNS injury: lack of axonal dieback and enhanced sprouting within the inhibitory environment of the glial scar. J Neurosci 31:5605–5616.

Holmes GM, Van Meter MJ, Beattie MS, Bresnahan JC (2005) Serotonergic fiber sprouting to external anal sphincter motoneurons after spinal cord contusion. Exp Neurol 193:29–42.

Hoshino Y, Nishide K, Nagoshi N, Shibata S, Moritoki N, Kojima K, Tsuji O, Matsumoto M, Kohyama J, Nakamura M, Okano H (2019) The adeno-associated virus rh10 vector is an effective gene transfer system for chronic spinal cord injury. Sci Rep 9:9844.

Hunanyan AS, Garcia-Alias G, Alessi V, Levine JM, Fawcett JW, Mendell LM, Arvanian VL (2010) Role of chondroitin sulfate proteoglycans in axonal conduction in mammalian spinal cord. J Neurosci 30:7761–7769.

Hunanyan AS, Alessi V, Patel S, Pearse DD, Matthews G, Arvanian VL (2011) Alterations of action potentials and the localization of Nav1.6 sodium channels in spared axons after hemisection injury of the spinal cord in adult rats. J Neurophysiol 105:1033–1044.

Hunanyan AS, Petrosyan HA, Alessi V, Arvanian VL (2012) Repetitive spinal electromagnetic stimulation opens a window of synaptic plasticity in damaged spinal cord: role of NMDA receptors. J Neurophysiol 107:3027–3039.

Hunanyan AS, Petrosyan HA, Alessi V, Arvanian VL (2013) Combination of chondroitinase ABC and AAV-NT3 promotes neural plasticity at descending spinal pathways after thoracic contusion. J Neurophysiol 110:1782–1792.

Jones LL, Yamaguchi Y, Stallcup WB, Tuszynski MH (2002) NG2 is a major chondroitin sulfate proteoglycan produced after spinal cord injury and is expressed by macrophages and oligodendrocyte progenitors. J Neurosci 22:2792–2803.

Kim BG, Dai HN, Lynskey JV, McAtee M, Bregman BS (2006) Degradation of chondroitin sulfate proteoglycans potentiates transplant-mediated axonal remodeling and functional recovery after spinal cord injury in adult rats. J Comp Neurol 497:182–198.

Kilcoyne M, Sharma S, McDevitt N, O'Leary C, Joshi L, McMahon SS (2012) Neuronal glycosylation differentials in normal, injured and chondroitinase-treated environments. Biochem Biophys Res Commun 420:616–622.

Kocsis JD, Waxman SG (1982) Intra-axonal recordings in rat dorsal column axons: membrane hyperpolarization and decreased excitability precede the primary afferent depolarization. Brain Res 238:222–227.

Koopmans GC, Deumens R, Honig WM, Hamers FP, Steinbusch HW, Joosten EA (2005) The assessment of locomotor function in spinal cord injured rats. J Neurotrauma 22:214–225.

Kwok JC, Warren P, Fawcett JW (2012) Chondroitin sulfate: a key molecule in the brain matrix. Int J Biochem Cell Biol 44:582–586.

LaPallo BK, Wolpaw JR, Chen XY, Carp JS (2017) Spinal transection alters external urethral sphincter activity during spontaneous voiding in freely moving rats. J Neurotrauma 34:3012–3026.

Lee H, McKeon RJ, Bellamkonda RV (2010) Sustained delivery of thermostabilized chABC enhances axonal sprouting and functional recovery after spinal cord injury. Proc Natl Acad Sci USA 107:3340–3345.

Levine JM (1994) Increased expression of the NG2 proteoglycan after brain injury. J Neurosci 14:4716–4730.

Margolis RK, Margolis RU (1993) Nervous tissue proteoglycans. Experientia 49:429–446.

Massey JM, et al. (2008) Increased chondroitin sulfate proteoglycan expression in denervated brainstem targets following spinal cord injury creates a barrier to axonal regeneration overcome by chondroitinase ABC and neurotrophin-3. Exp Neurol 209:426–445.

McKeon RJ, Schreiber RC, Rudge JS, Silver J (1991) Reduction of neurite outgrowth in a model of glial scarring following CNS injury is correlated with the expression of inhibitory molecules on reactive astrocytes. J Neurosci 11:3398–3411.

Mendell LM, Munson JB, Arvanian VL (2001) Neurotrophins and synaptic plasticity in the mammalian spinal cord. J Physiol 533:91–97.

Moon LD, Asher RA, Rhodes KE, Fawcett JW (2001) Regeneration of CNS axons back to their target following treatment of adult rat brain with chondroitinase ABC. Nat Neurosci 4:465–466.

Murray M, Fischer I, Smeraski C, Tessler A, Giszter S (2004) Towards a definition of recovery of function. J Neurotrauma 21:405–413.

Nishiyama A, Dahlin KJ, Prince JT, Johnstone SR, Stallcup WB (1991) The primary structure of NG2, a novel membrane-spanning proteoglycan. J Cell Biol 114:359–371.

Novak KR, Nardelli P, Cope TC, Filatov G, Glass JD, Khan J, Rich MM (2009) Inactivation of sodium channels underlies reversible neuropathy during critical illness in rats. J Clin Invest 119:1150–1158.

Pearse DD, Lo TP Jr, Cho KS, Lynch MP, Garg MS, Marcillo AE, Sanchez AR, Cruz Y, Dietrich WD (2005) Histopathological and behavioral characterization of a novel cervical spinal cord displacement contusion injury in the rat. J Neurotrauma 22:680–702.

Petrosyan HA, Hunanyan AS, Alessi V, Schnell L, Levine J, Arvanian VL (2013) Neutralization of inhibitory molecule NG2 improves synaptic transmission, retrograde transport, and locomotor function after spinal cord injury in adult rats. J Neurosci 33:4032–4043.

Petrosyan HA, Alessi V, Singh V, Hunanyan AS, Levine JM, Arvanian VL (2014) Transduction efficiency of neurons and glial cells by AAV-1-10 serotypes in rat spinal cord following contusion injury. Gene Ther 21:991–1000.

Petrosyan HA, Alessi V, Hunanyan AS, Sisto SA, Arvanian VL (2015) Spinal electro-magnetic stimulation combined with transgene delivery of neurotrophin NT-3 and exercise: novel combination therapy for spinal contusion injury. J Neurophysiol 114:2923–2940.

Ruitenberg MJ, Blits B, Dijkhuizen PA, te Beek ET, Bakker A, van Heerikhuize JJ, Pool CW, Hermens WT, Boer GJ, Verhaagen J (2004) Adeno-associated viral vector-mediated gene transfer of brain-derived neurotrophic factor reverses atrophy of rubrospinal neurons following both acute and chronic spinal cord injury. Neurobiol Dis 15:394–406.

Sakry D, Neitz A, Singh J, Frischknecht R, Marongiu D, Binamé F, Perera SS, Endres K, Lutz B, Radyushkin K, Trotter J, Mittmann T (2014) Oligodendrocyte precursor cells modulate the neuronal network by activity-dependent ectodomain cleavage of glial NG2. PLoS Biol 12:e1001993.

Saruhashi Y, Young W, Perkins R (1996) The recovery of 5-HT immunoreactivity in lumbosacral spinal cord and locomotor function after thoracic hemisection. Exp Neurol 139:203–213.

Schnell L, et al. (1994) Neurotrophin-3 enhances sprouting of corticospinal tract during development and after adult spinal cord lesion. Nature 367:170–173.

Schnell L, Hunanyan AS, Bowers WJ, Horner PJ, Federoff HJ, Gullo M, Schwab ME, Mendell LM, Arvanian VL (2011) Combined delivery of Nogo-A antibody, neurotrophin-3 and the NMDA-NR2d subunit establishes a functional 'detour' in the hemisected spinal cord. Eur J Neurosci 34:1256–1267.

Serwanski DR, Jukkola P, Nishiyama A (2017) Heterogeneity of astrocyte and NG2 cell insertion at the node of Ranvier. J Comp Neurol 525:535–552.

Siegenthaler MM, Tu MK, Keirstead HS (2007) The extent of myelin pathology differs following contusion and transection spinal cord injury. J Neurotrauma 24:1631–1646.

Silver J, Miller JH (2004) Regeneration beyond the glial scar. Nat Rev Neurosci 5:146–156.

Snow DM, Lemmon V, Carrino DA, Caplan AI, Silver J (1990) Sulfated proteoglycans in astroglial barriers inhibit neurite outgrowth in vitro. Exp Neurol 109:111–130.

Stallcup WB (2002) The NG2 proteoglycan: past insights and future prospects. J Neurocytol 31:423–435.

Tan AM, Colletti M, Rorai AT, Skene JH, Levine JM (2006) Antibodies against the NG2 proteoglycan promote the regeneration of sensory axons within the dorsal columns of the spinal cord. J Neurosci 26:4729–4739.

Tom VJ, Kadakia R, Santi L, Houlé JD (2009) Administration of chondroitinase ABC rostral or caudal to a spinal cord injury site promotes anatomical but not functional plasticity. J Neurotrauma 26:2323–2333.

Tuszynski MH, Gage FH (1995) Maintaining the neuronal phenotype after injury in the adult CNS. Neurotrophic factors, axonal growth substrates, and gene therapy. Mol Neurobiol 10:151–167.

Ughrin Y, Chen ZJ, Levine JM (2003) Domains of NG2 mediate axon growth inhibition. J Neurosci 23:175–186.

Wang X, Messing A, David S (1997) Axonal and nonneuronal cell responses to spinal cord injury in mice lacking glial fibrillary acidic protein. Exp Neurol 148:568–576.

Ward PJ, Herrity AN, Smith RR, Willhite A, Harrison BJ, Petruska JC, Harkema SJ, Hubscher CH (2014) Novel multi-system functional gains via task specific training in spinal cord injured male rats. J Neurotrauma 31:819–833.

Williams RR, Pearse DD, Tresco PA, Bunge MB (2012) The assessment of adeno-associated vectors as potential intrinsic treatments for brainstem axon regeneration. J Gene Med 14:20–34.

Yamagata T, Saito H, Habuchi O, Suzuki S (1968) Purification and properties of bacterial chondroitinases and chondrosulfatases. J Biol Chem 243:1523–1535.

Yiu G, He Z (2006) Glial inhibition of CNS axon regeneration. Nat Rev Neurosci 7:617–627.

Zhou X, et al. (2001) Neurocan is dispensable for brain development. Mol Cell Biol 21:5970–5978.

Zhou X, Wahane S, Friedl MS, Kluge M, Friedel CC, Avrampou K, Zachariou V, Guo L, Zhang B, He X, Friedel RH, Zou H (2020) Microglia and macrophages promote corralling, wound compaction and recovery after spinal cord injury via Plexin-B2. Nat Neurosci 23:337–350.